



**HAL**  
open science

## Experimental study of the formation of organosulfates from $\alpha$ -Pinene oxidation. 2. Time evolution and effect of particle acidity

Geoffroy Duporté, Pierre-Marie Flaud, Julien Kammer, Emmanuel Geneste, Sylvie Augagneur, Edouard Pangui, Houssni Lamkaddam, Aline Gratien, Jean-François Doussin, Hélène Budzinski, et al.

### ► To cite this version:

Geoffroy Duporté, Pierre-Marie Flaud, Julien Kammer, Emmanuel Geneste, Sylvie Augagneur, et al.. Experimental study of the formation of organosulfates from  $\alpha$ -Pinene oxidation. 2. Time evolution and effect of particle acidity. *Journal of Physical Chemistry A*, 2020, 124 (2), pp.409-421. 10.1021/acs.jpca.9b07156 . hal-02967567

**HAL Id: hal-02967567**

**<https://hal.science/hal-02967567v1>**

Submitted on 8 Oct 2024

**HAL** is a multi-disciplinary open access archive for the deposit and dissemination of scientific research documents, whether they are published or not. The documents may come from teaching and research institutions in France or abroad, or from public or private research centers.

L'archive ouverte pluridisciplinaire **HAL**, est destinée au dépôt et à la diffusion de documents scientifiques de niveau recherche, publiés ou non, émanant des établissements d'enseignement et de recherche français ou étrangers, des laboratoires publics ou privés.

A: Environmental, Combustion, and Atmospheric Chemistry; Aerosol Processes, Geochemistry, and Astrochemistry

## Experimental Study of the Formation of Organosulfates From #-Pinene Oxidation. Part II : Time Evolution and Effect of Particle Acidity

Geoffroy DUPORTE, Pierre-Marie Flaud, Julien Kammer, Emmanuel Geneste, Sylvie Augagneur, Edouard Pangui, Houssni Lamkaddam, Aline Gratien, Jean-Francois Doussin, Helene Budzinski, Eric VILLENAVE, and Emilie Perraudin

*J. Phys. Chem. A*, **Just Accepted Manuscript** • DOI: 10.1021/acs.jpca.9b07156 • Publication Date (Web): 18 Dec 2019

Downloaded from [pubs.acs.org](https://pubs.acs.org) on December 22, 2019

### Just Accepted

“Just Accepted” manuscripts have been peer-reviewed and accepted for publication. They are posted online prior to technical editing, formatting for publication and author proofing. The American Chemical Society provides “Just Accepted” as a service to the research community to expedite the dissemination of scientific material as soon as possible after acceptance. “Just Accepted” manuscripts appear in full in PDF format accompanied by an HTML abstract. “Just Accepted” manuscripts have been fully peer reviewed, but should not be considered the official version of record. They are citable by the Digital Object Identifier (DOI®). “Just Accepted” is an optional service offered to authors. Therefore, the “Just Accepted” Web site may not include all articles that will be published in the journal. After a manuscript is technically edited and formatted, it will be removed from the “Just Accepted” Web site and published as an ASAP article. Note that technical editing may introduce minor changes to the manuscript text and/or graphics which could affect content, and all legal disclaimers and ethical guidelines that apply to the journal pertain. ACS cannot be held responsible for errors or consequences arising from the use of information contained in these “Just Accepted” manuscripts.

1  
2  
3  
4 1 Experimental study of the formation of organosulfates  
5  
6  
7 2 from  $\alpha$ -pinene oxidation. Part II: Time evolution and  
8  
9  
10 3 effect of particle acidity  
11  
12

13 4 *G. Duporté<sup>a,b</sup>, P.-M. Flaud<sup>a,b</sup>, J. Kammer<sup>a,b,#</sup>, E. Geneste<sup>a,b</sup>, S. Augagneur<sup>a,b</sup>, E. Pangui<sup>c</sup>, H.*  
14  
15  
16 5 *Lamkaddam<sup>c,†</sup>, A. Gratien<sup>c</sup>, J.-F. Doussin<sup>c</sup>, H. Budzinski<sup>a,b</sup>, E. Villenave<sup>a,b</sup> and E. Perraudin<sup>a,b\*</sup>*  
17  
18

19 6 *<sup>a</sup>Université de Bordeaux, EPOC, UMR 5805, F-33405 Talence Cedex, France*  
20  
21

22 7 *<sup>b</sup>CNRS, EPOC, UMR 5805, F-33405 Talence Cedex, France*  
23  
24

25  
26 8 *<sup>c</sup>Université Paris-Est-Créteil (UPEC) and Université Paris Diderot (UPD), LISA, UMR 7583, F-*  
27  
28 9 *94010 Créteil, France*

29  
30  
31 10 *<sup>†</sup>Now at Paul Scherrer Institute, Laboratory of Atmospheric Chemistry, 5232 Villigen PSI,*  
32  
33 11 *Switzerland*

34  
35  
36 12 *<sup>#</sup>Now at LSCE, UMR 8212 CEA-CNRS-UVSQ, IPSL, University Paris-Saclay, 91191 Gif-sur-Yvette,*  
37  
38 13 *France*

39  
40 14  
41 15 *\* corresponding author*  
42

43  
44 16 *Tel.: +33 5 4000 2868 E-mail address: [emilie.perraudin@u-bordeaux.fr](mailto:emilie.perraudin@u-bordeaux.fr)*  
45  
46

## Abstract

The present work is an extensive laboratory study of organosulfate (OS) formation from the reaction of  $\alpha$ -pinene oxidation products or proxies with acidified ammonium sulfate aerosols in three different acidity conditions ( $(\text{NH}_4)_2\text{SO}_4$  0.06 M;  $(\text{NH}_4)_2\text{SO}_4/\text{H}_2\text{SO}_4$  0.06 M/0.005 M;  $(\text{NH}_4)_2\text{SO}_4/\text{H}_2\text{SO}_4$  0.03 M/0.05 M). The kinetics of the reactions of  $\alpha$ -pinene,  $\alpha$ -pinene oxide, isopinocampheol, pinanediol and myrtenal with ammonium sulfate particles were studied using a quasi-static reactor. The reaction of  $\alpha$ -pinene oxide with the highly acidic ammonium sulfate particles was determined to be 7, 10, 21 and 24 times faster than for isopinocampheol,  $\alpha$ -pinene, pinanediol and myrtenal, respectively for an OS precursor concentration of 1 ppm and after 1h reaction time. The effective rate coefficients for OS formation from  $\alpha$ -pinene oxide were determined to be two orders of magnitude higher in highly acidic conditions than for the two other acidity conditions. For  $\alpha$ -pinene oxide reactions with highly acidic ammonium sulfate particles, OS formation was observed to increase linearly with (i) the time of reaction up to 400 minutes ( $r^2 > 0.95$ ) and (ii)  $\alpha$ -pinene oxide gas-phase concentration. However, OS formation from  $\alpha$ -pinene oxide reactions with slightly acidic or pure ammonium sulfate particles was limited, with a plateau ( $[\text{OS}]_{\text{max}} = 0.62 \pm 0.03 \mu\text{g}$ ) reached after around 15-20 minutes. Organosulfate dimers ( $m/z$  401 and  $m/z$  481) were detected not only with highly acidic particles but also with slightly acidic and pure ammonium sulfate particles, indicating that oligomerization processes do not require strong acidity conditions. Dehydration products of organosulfates ( $m/z$  231 and  $m/z$  383) were observed only under highly acidic conditions, indicating the key role of  $\text{H}_2\text{SO}_4$  on the dehydration of organosulfates and the formation of olefins in the atmosphere. Finally, this kinetic study was completed with simulation chamber experiments in which mass concentration of organosulfates was shown to depend on the available sulfate amount present in the particle phase ( $r^2 = 0.96$ ). In conclusion, this relative comparison between 5 organosulfate precursors shows that epoxide was the most efficient reactant to form organosulfates via heterogeneous gas-particle reactions and illustrates how gas-particle reactions may play an important role in OS formation and hence in the atmospheric fate of organic carbon. The kinetic data presented in this work provides strong support to organosulfate formation mechanisms proposed in the companion paper.

## 52 Introduction

53 Atmospheric particulate matter (PM) is known to play a key role in affecting climate change and air quality,  
54 leading to adverse health impact.<sup>1-4</sup> Atmospheric oxidation of biogenic volatile organic compounds (BVOCs)  
55 play a significant role in the formation of secondary organic aerosols (SOAs).<sup>4</sup> Biogenic secondary organic  
56 aerosols (BSOAs) contribute to a significant mass fraction of the fine particulate matter (PM<sub>2.5</sub>) measured in  
57 several locations.<sup>4</sup> Despite ongoing improvements and the use of more sophisticated techniques, the  
58 insufficient knowledge of the composition of organic aerosol particles at the molecular level hinders a better  
59 understanding of the sources, formation and atmospheric processes of organic aerosol.<sup>5</sup>

60 Organosulfates (OSs) are ubiquitous in atmospheric aerosol particles and have been detected in ambient  
61 aerosols in various sites around the world.<sup>6-21</sup> OSs have been identified in laboratory experiments in the  
62 presence of acidified sulfate aerosol from various VOCs including isoprene,<sup>6,22</sup> monoterpenes,<sup>6,7,22-24</sup>  
63 sesquiterpenes,<sup>25</sup> polycyclic aromatic hydrocarbons,<sup>8</sup> or alkanes.<sup>26</sup> These studies have shown the key role of  
64 acidity in enhancing both SOA and OS formation. OSs may represent an important fraction of ambient organic  
65 aerosols, estimated to contribute up to 30 % of the PM<sub>10</sub> organic mass.<sup>22,27</sup> Their highly oxygenated and sulfated  
66 chemical structure suggests that their presence may modify aerosol hygroscopicity leading to larger potential  
67 climate impact through formation of cloud condensation nuclei (CCN).<sup>28</sup> OS formation mechanisms have also  
68 been proposed in laboratory studies for oxidized BVOCs such as pinonaldehyde,<sup>29</sup> glyoxal,<sup>30</sup>  $\alpha$ -pinene  
69 oxide,<sup>23,24</sup>  $\beta$ -pinene oxide,<sup>23</sup> isoprene epoxydiols (IEPOX),<sup>31,32</sup> or pinanediol.<sup>24</sup> During the last decade, a  
70 particular attention has been paid to epoxide compounds and related studies have highlighted that  
71 organosulfates are most likely formed from acid-catalysed reaction of epoxides with inorganic sulfate aerosol.  
72 <sup>20,22,30-37</sup> Few kinetic studies of organosulfate formation were conducted<sup>33-35</sup> and it was found experimentally  
73 in bulk aqueous solutions that epoxide reactions with sulfuric acid are kinetically favored over those of alcohols  
74 or aldehydes.<sup>34,36,37</sup> Kinetics studies of the aqueous-phase reactions of several monoterpenes epoxides (i.e.  $\alpha$ -  
75 pinene oxide,  $\beta$ -pinene oxide, limonene oxide) have demonstrated that all of these epoxides will react more  
76 rapidly than isoprene epoxydiols in aqueous atmospheric particles, even under low-acidity conditions.<sup>35,38</sup>  
77 Some organosulfate formation pathways have been proposed in these studies, such as the esterification of  
78 hydroxyl or keto groups,<sup>28,29</sup> the acid-catalyzed ring-opening of epoxides,<sup>23,34,36,39</sup> radical-initiated processes in

1  
2  
3 79 aqueous aerosols,<sup>40,41</sup> or the nucleophilic substitution of organonitrates.<sup>33</sup> It is now crucial to gain further  
4  
5 80 insights into mechanistic and kinetic processes describing OS formation.  
6  
7

8 81 In a recent companion study,<sup>24</sup> a new experimental approach has been described to perform simple and various  
9  
10 82 experiments under controlled and repeatable conditions, to study heterogeneous processes at the gas-particle  
11  
12 83 interface. Mechanisms describing organosulfate formation from  $\alpha$ -pinene,  $\alpha$ -pinene oxide, isopinocampheol,  
13  
14 84 myrtenal and pinanediol have been proposed. Here, an extensive kinetic study of organosulfate formation from  
15  
16 85  $\alpha$ -pinene oxide reactions with acidified ammonium sulfate aerosol was performed using a quasi-static reactor  
17  
18 86 in quasi-dry conditions. These simplified experimental conditions were selected to specifically investigate the  
19  
20 87 gas-surface reaction of a series of oxygenated VOCs with sulfate particles as a first step of the multiphase  
21  
22 88 process of reactive uptake. Kinetics information on heterogeneous formation of organosulfates was  
23  
24 89 investigated, for the first time, with this approach in complement to previous studies focused on bulk  
25  
26 90 reactions.<sup>33–38,42</sup> Effect of particle acidity on organosulfate formation is discussed. Complementary experiments  
27  
28 91 in more atmospherically relevant conditions were performed in an atmospheric simulation chamber. In both  
29  
30 92 experimental approaches, the gaseous phase was characterized by Proton Transfer Reactor - Time of Flight -  
31  
32 93 Mass Spectrometer (PTR-TOF-MS). Organosulfate formation in the particle-phase was investigated by Liquid  
33  
34 94 Chromatography combined with Electrospray Ionization (ESI) Mass Spectrometry (LC/ESI-MS) or with ESI  
35  
36 95 High-Resolution – Time of Flight - Mass Spectrometry (LC/ESI-HR-QTOFMS) for structural elucidation. In  
37  
38 96 this work, time evolutions of organosulfate formation from four other BVOCs ( $\alpha$ -pinene, isopinocampheol,  
39  
40 97 pinanediol and myrtenal) are also presented and compared.  
41  
42  
43  
44  
45 98

## 48 99 **Experimental section**

### 51 100 **Quasi-static reactor experiments**

53 101 The experimental approach using a quasi-static reactor was developed to the study of heterogeneous processes  
54  
55 102 at the gas-particle interface. The experimental set-up and procedure were described in detail and fully validated  
56  
57 103 in the recent companion article.<sup>24</sup> With this set-up, heterogeneous reactions were investigated under pseudo-  
58  
59 104 first order conditions, as demonstrated in each experiment by on-line monitoring of the gas phase composition

1  
2  
3  
4  
5  
6  
7  
8  
9  
10  
11  
12  
13  
14  
15  
16  
17  
18  
19  
20  
21  
22  
23  
24  
25  
26  
27  
28  
29  
30  
31  
32  
33  
34  
35  
36  
37  
38  
39  
40  
41  
42  
43  
44  
45  
46  
47  
48  
49  
50  
51  
52  
53  
54  
55  
56  
57  
58  
59  
60

105 using PTR-TOF-MS. Briefly, experiments are based on the exposure of aerosols, deposited on a filter in a  
106 quasi-static reactor, to a continuous flow of a single volatile organic compound (VOC) under pseudo-first order  
107 conditions. VOC flow was generated by flushing nitrogen ( $N_2$ ) into a bubbler of pure liquid compound. The  
108 VOC concentration (0.1 – 10 ppm) was then diluted in oxygen ( $O_2$ ) and  $N_2$ , with a final  $O_2$  concentration near  
109 20 % of the mixture.  $O_2$  (99.9990 % purity, Linde Gas SA) and  $N_2$  (99.9990 % purity, Linde Gas SA) flows  
110 were controlled using mass flow controllers. Reactions were performed in complete darkness, at atmospheric  
111 pressure and ambient temperature ( $295 \pm 2$  K). The detailed experimental conditions are given in Table 1.  
112 Inorganic aerosols were generated by atomizing (using a TSI model 3075 through a diffusion dryer (TSI, model  
113 3062)) an aqueous solution containing the seed aerosol constituents as presented in Table 1 and were collected  
114 on 47-mm PTFE filters (Millipore, Fluoropore<sup>TM</sup>, 0.2  $\mu m$  FG). The three different aerosol acidities were  
115 generated by varying the composition of the atomization solutions to investigate the effect of aerosol acidity  
116 on organosulfate formation. Prior to experiments, particles were further dried during an optimized 5 min-  
117 exposure to an orthogonal 1 L  $min^{-1}$  flow of nitrogen. The drying efficiency of the procedure was controlled  
118 by weighting the particles (on a filter). The drying step was considered to be achieved when the particle mass  
119 was checked to be stable within the instrumental uncertainty of a daily calibrated microbalance (i.e. 0,0001 g  
120 corresponding to 2-3 % of the total particle mass).

121 Experiments were thus considered to be performed in quasi-dry conditions ( $RH < 1 \pm 1$  %). Meanwhile, it  
122 should be specified that a small residual amount of water may still be present in the particles, especially in the  
123 case of acidified particles due to the well-known strong hygroscopic properties of sulfuric acid.

**Table 1. Experimental conditions of organosulfate formation in the quasi-static reactor for kinetic study. HA : highly acidic aerosols, SA : slightly acidic aerosols, NA : non-acidified aerosols**

VOC	no. of experiment series	[VOC] (ppm)	Inorganic aerosol	Composition of atomized solution (M)	Acidity conditions	T (K)	Reaction time (min) (n experiments)
$\alpha$ -pinene oxide	R0	3.30 $\pm$ 0.1	(NH <sub>4</sub> ) <sub>2</sub> SO <sub>4</sub> /H <sub>2</sub> SO <sub>4</sub>	0.03/0.05	HA	295 $\pm$ 2	0-400 (n = 37)
$\alpha$ -pinene oxide	R1	1.00 $\pm$ 0.02	(NH <sub>4</sub> ) <sub>2</sub> SO <sub>4</sub> /H <sub>2</sub> SO <sub>4</sub>	0.03/0.05		295 $\pm$ 2	0-200 (n = 8)
$\alpha$ -pinene oxide	R6	3.30 $\pm$ 0.1	(NH <sub>4</sub> ) <sub>2</sub> SO <sub>4</sub> /H <sub>2</sub> SO <sub>4</sub>	0.06/0.005	SA	295 $\pm$ 2	0-90 (n = 43)
$\alpha$ -pinene oxide	R7	1.65 $\pm$ 0.03	(NH <sub>4</sub> ) <sub>2</sub> SO <sub>4</sub> /H <sub>2</sub> SO <sub>4</sub>	0.06/0.005		295 $\pm$ 2	0-90 (n = 13)
$\alpha$ -pinene oxide	R8	0.82 $\pm$ 0.02	(NH <sub>4</sub> ) <sub>2</sub> SO <sub>4</sub> /H <sub>2</sub> SO <sub>4</sub>	0.06/0.005		295 $\pm$ 2	0-90 (n = 10)
$\alpha$ -pinene oxide	R9	0.33 $\pm$ 0.02	(NH <sub>4</sub> ) <sub>2</sub> SO <sub>4</sub> /H <sub>2</sub> SO <sub>4</sub>	0.06/0.005		295 $\pm$ 2	0-60 (n = 5)
$\alpha$ -pinene oxide	R10	3.30 $\pm$ 0.1	(NH <sub>4</sub> ) <sub>2</sub> SO <sub>4</sub>	0.06	NA	295 $\pm$ 2	0-60 (n = 16)
$\alpha$ -pinene	R2	1.00 $\pm$ 0.02	(NH <sub>4</sub> ) <sub>2</sub> SO <sub>4</sub> /H <sub>2</sub> SO <sub>4</sub>	0.03/0.05	HA	295 $\pm$ 2	0-90 (n = 7)
isopinocampheol	R3	1.00 $\pm$ 0.02	(NH <sub>4</sub> ) <sub>2</sub> SO <sub>4</sub> /H <sub>2</sub> SO <sub>4</sub>	0.03/0.05	HA	295 $\pm$ 2	0-90 (n = 7)
pinanediol	R4	1.00 $\pm$ 0.02	(NH <sub>4</sub> ) <sub>2</sub> SO <sub>4</sub> /H <sub>2</sub> SO <sub>4</sub>	0.03/0.05	HA	295 $\pm$ 2	0-90 (n = 7)
myrtenal	R5	1.00 $\pm$ 0.02	(NH <sub>4</sub> ) <sub>2</sub> SO <sub>4</sub> /H <sub>2</sub> SO <sub>4</sub>	0.03/0.05	HA	295 $\pm$ 2	0-60 (n = 6)

After generation via aqueous solution atomization and drying using an aerosol diffusion dryer (TSI 3062), inorganic seed aerosols, deposited on a filter, were introduced in the reaction cell and exposed to the VOC/O<sub>2</sub>/N<sub>2</sub> flow for a specific reaction time. The gas-phase constituents were monitored by PTR-TOF-MS (Kore Technology) all along the experiments. At the end of the reaction, the cell was purged with N<sub>2</sub> and aerosols were recovered, extracted and dissolved in 3 mL of acetonitrile (ACN) by sonification during 15 min in the presence of an internal standard, stored at - 18 °C and analyzed within 3 months.

### Chamber experiments

Organosulfate formation from  $\alpha$ -pinene oxide reactions was also studied in more atmospherically relevant conditions in the CESAM chamber (French acronym for Experimental Multiphase Atmospheric Simulation Chamber). The CESAM chamber was designed to study multiphase atmospheric (photo-)chemistry and has been described in detail elsewhere.<sup>43</sup> Briefly, this facility consists of a cylindrical 4.2 m<sup>3</sup> double walled stainless steel chamber. Both temperature and relative humidity (RH) were measured with HMP234 Vaisala® humidity and temperature transmitter equipped with a capacitive thin film polymer sensor Humicap®. The circulation of



1  
2  
3 148 a cooling liquid at a suitable temperature regulated by a 10 kW thermostat (LAUDA, Integral T10000 W) was  
4  
5 149 allowed to circulate between the double walls of the chamber in order to maintain the inner temperature during  
6  
7 150 the experiment in the range (293 – 295) K between experiment, with a stability better than 1 K within the course  
8  
9 151 of a single experiment (Table 1).

11  
12 152 Experiments were carried out under dark conditions and at atmospheric pressure. Initial experimental  
13  
14 153 conditions are described in Table 2. Between each experiment, the chamber was cleaned by maintaining a  
15  
16 154 secondary vacuum ( $\sim 6 \times 10^{-4}$  hPa) overnight. The chamber was then filled with synthetic air produced from  
17  
18  
19 155 a mixture of  $\sim 200$  hPa of O<sub>2</sub> (Air Liquide, Alphagaz class 1) and  $\sim 800$  hPa of N<sub>2</sub> generated from the  
20  
21 156 evaporation of pressurized liquid nitrogen (Messer, purity > 99.995%). Inorganic seed aerosols were  
22  
23 157 introduced into the chamber by atomizing (using a TSI model 3075 through a diffusion dryer (TSI, model  
24  
25 158 3062)) a solution containing the seed aerosol constituents presented in Table 2. Particle size distributions (20-  
26  
27 159 980 nm diameter) were measured with a Scanning Mobility Particle Sizer (SMPS) composed of a TSI 3080  
28  
29 160 Differential Mobility Analyzer (DMA) and a TSI 3010 Condensation Particle Counter (CPC), assuming a  
30  
31 161 particle density of 1 g cm<sup>-3</sup>. Then, injection of  $\alpha$ -pinene oxide (Sigma-Aldrich, 97 % purity) was performed by  
32  
33 162 introducing a precisely known partial pressure of the compound ( $\pm 0.1$  mbar) prepared in a bulb of known  
34  
35 163 volume ( $V = 2.90516$  L) from a frozen pure standard solution using a vacuum gas manifold. The bulb content  
36  
37  
38 164 was then immediately flushed with N<sub>2</sub> into the chamber. The concentration of  $\alpha$ -pinene oxide was monitored  
39  
40 165 using a Fourier-Transform Infrared Spectrometer (FTIR) from Bruker™ Tensor 37®. The total optical path  
41  
42 166 length for the in-situ FTIR measurements was set to 192 m. In addition to FTIR, the gas-phase composition  
43  
44 167 was also monitored by a PTR-TOF-MS from Kore Technology. Each reaction was studied for 3 hours. The  
45  
46 168 mass concentration data from the experiments performed in the CESAM chamber were treated using a new  
47  
48 169 algorithm developed recently by Lamkaddam et al.<sup>44</sup> The data could be corrected for both the dilution and the  
49  
50 170 aerosol physical wall losses. These wall losses were corrected using a size dependent deposition rate coefficient  
51  
52 171 parameterized using the model proposed by Lai and Nazaroff.<sup>45</sup>

53  
54  
55 172 Temporal profiles of organosulfate formation were investigated by collecting filters sampled every 25 min  
56  
57 173 throughout the experiments (6 filters collected and labelled F<sub>1</sub>-F<sub>6</sub>). In parallel, organosulfate formation was  
58  
59 174 also characterized by a filter sample collected over the entire time of the experiments (labelled F<sub>tot</sub>). Aerosol

sampling was achieved by using 47-mm PTFE filters (Millipore, Fluoropore™, 0.2 μm FG). Before the VOC injection, inorganic seed aerosols were collected during 25 min onto a blank filter. The filter holders were installed downstream of an activated charcoal denuder, which was used to trap reactive gases and reduce positive sampling artefacts. The filter collection was performed at a flow rate of 3 L min<sup>-1</sup>. The filters were extracted in 3 mL of ACN during 15 min of ultrasonic agitation and the final extracts were kept at -18°C and analyzed within 3 months.

**Table 2. Summary of chamber experiment initial conditions; HA : highly acidic particles, SA : slightly acidic particles, NA : non-acidified particles**

Experiment #	Hydrocarbon	Initial [VOC] (ppb)	Seed aerosol	Composition of atomized solution (M)	Acidity conditions	Initial seed particle mass (μg m <sup>-3</sup> )	T (K)	RH (%)
C1	α-pinene oxide	117	(NH <sub>4</sub> ) <sub>2</sub> SO <sub>4</sub> /H <sub>2</sub> SO <sub>4</sub>	0.03/0.05	HA	18.5	294 ± 1	< 1 ± 1
C4	α-pinene oxide	116	(NH <sub>4</sub> ) <sub>2</sub> SO <sub>4</sub> /H <sub>2</sub> SO <sub>4</sub>	0.003/0.005	HA	23	293 ± 1	< 1 ± 1
C7	α-pinene oxide	116	(NH <sub>4</sub> ) <sub>2</sub> SO <sub>4</sub> /H <sub>2</sub> SO <sub>4</sub>	0.06/0.005	SA	25	294 ± 1	< 1 ± 1
C8	α-pinene oxide	132	(NH <sub>4</sub> ) <sub>2</sub> SO <sub>4</sub>	0.06	NA	19	295 ± 1	< 1 ± 1

### Sample preparation and analysis

The detailed extraction procedure and operating conditions of the analytical method have been previously described in the companion article<sup>24</sup> and hence, will only be presented briefly here.

As described above, filter samples were extracted in 3 mL of acetonitrile (HPLC Grade, JT Baker) during 15 min of ultrasonic agitation. Then, extracts were filtered by centrifugation using PTFE filters (Ultrafree-MC, PTFE Membrane, 0.22 μm) and concentrated to about 50 μL under a gentle N<sub>2</sub> stream (99.995 % purity, Linde Gas SA) at 40 °C. Syringe standard (Octanoic acid <sup>13</sup>C, Isotec, 99 %) was added to the samples for quantification of the internal standard before analysis. This double quantification allows the calculation of internal standard recovery yields and hence to check that internal standards, and therefore organosulfates, are not lost along the analytical workup procedures. Internal standard recovery yields were higher than 80 % for all samples analyzed in the present work. Filter extracts were analyzed by LC/ESI-MS and by HPLC(-)ESI-HR-QTOFMS. Chromatographic conditions and mass spectrometry parameters have already been presented

1  
2  
3  
4  
5  
6  
7  
8  
9  
10  
11  
12  
13  
14  
15  
16  
17  
18  
19  
20  
21  
22  
23  
24  
25  
26  
27  
28  
29  
30  
31  
32  
33  
34  
35  
36  
37  
38  
39  
40  
41  
42  
43  
44  
45  
46  
47  
48  
49  
50  
51  
52  
53  
54  
55  
56  
57  
58  
59  
60

196 in the companion article.<sup>24</sup> All products were detected as their deprotonated ions (i.e.  $[M - H]^-$ ). Camphor  
197 sulfonic acid (Sigma Aldrich 98 %) was used as an internal standard for quantification of organosulfates due  
198 to the lack of commercially available authentic standards for organosulfates. Although the use of surrogate  
199 compounds adds some uncertainty to the absolute quantification of OS, it does provide access to reliable  
200 information on relative variations and time-trends.<sup>46</sup> Analyses were carried out only if the conditions required  
201 for analysis (absence of contamination in the blank samples, sensitivity and response factors within 15 % of  
202 the optimized conditions) were fulfilled. Calibration solutions were injected before each analysis sequence and  
203 about every 10 samples to calculate the internal standard response factors. Organosulfate functional groups  
204 were identified by LC/ESI-HR-QTOFMS from their fragmentation ions  $SO_3^-$  ( $m/z = 79.9574$ ),  $SO_4^-$  ( $m/z =$   
205  $95.9523$ ) or  $HSO_4^-$  ( $m/z = 96.9601$ ).

## 207 **Results and discussion**

208 As shown in the companion article<sup>24</sup>, the sum of organosulfates formed from  $\alpha$ -pinene oxide was much higher  
209 than from the other VOCs studied under similar experimental conditions. Thus, kinetic experiments focused  
210 here primarily on the  $\alpha$ -pinene oxide reaction. Temporal variations of organosulfate concentrations from other  
211 VOC experiments are also compared and discussed.

### 212 **Organosulfate formation from $\alpha$ -pinene oxide – Quasi-static reactor experiments**

#### 213 **Pseudo-first order conditions**

214 The gas phase concentration of  $\alpha$ -pinene oxide was checked to be constant by on-line monitoring using PTR-  
215 TOF-MS measurements along all experiments, demonstrating pseudo-first order kinetic conditions. Moreover,  
216 the total gas flow (dilution flow = 3.5 L min<sup>-1</sup> and  $\alpha$ -pinene oxide bubbler flow = 0.04 – 0.10 L min<sup>-1</sup>) in the  
217 reaction cell was always higher than 3.5 L min<sup>-1</sup>, leading to a VOC residence time in the reactor < 1 s,  
218 minimizing the VOC wall loss. Figure 1 presents the time monitoring of ions by PTR-TOF-MS at  $m/z$  153  
219 ( $C_{10}H_{17}O^+$ ), 135 ( $C_{10}H_{15}^+$ ) and 21 ( $H_3^{21}O^+$ ) in two experiments ( $t_{\text{reaction}} = 30$  min) performed (a) in highly acidic  
220 conditions and (b) in slightly acidic conditions. As presented in Figure S1a,  $m/z$  153 and  $m/z$  135 are  
221 characteristic PTR-TOF-MS fragments of  $\alpha$ -pinene oxide. Nonetheless, a change in the  $(m/z\ 153)/(m/z\ 135)$   
222 ratio was observed when highly acidic aerosols were exposed to gaseous  $\alpha$ -pinene oxide (Figure 1a). Alpha-  
223 pinene oxide isomerization reaction has already been evidenced in previous studies under acidic conditions,  
224 forming campholenic aldehyde.<sup>23,47</sup> The formation of campholenic aldehyde is highly suspected in this work  
225 but was not confirmed in the present experiments, both isomers (campholenic aldehyde and alpha-pinene  
226 oxide) having the same PTR-TOF-MS fragments under our experimental conditions (Figures S1a and S1b).  
227 Nonetheless, it is worth nothing that this different ratio is consistent with the observed different ion distribution  
228 for campholenic aldehyde, as shown in Figure S1. Under slightly acidic or neutral conditions, a change in the  
229  $(m/z\ 153) / (m/z\ 135)$  ratio was never observed, suggesting that the isomerization reaction is catalyzed under  
230 acidic conditions.

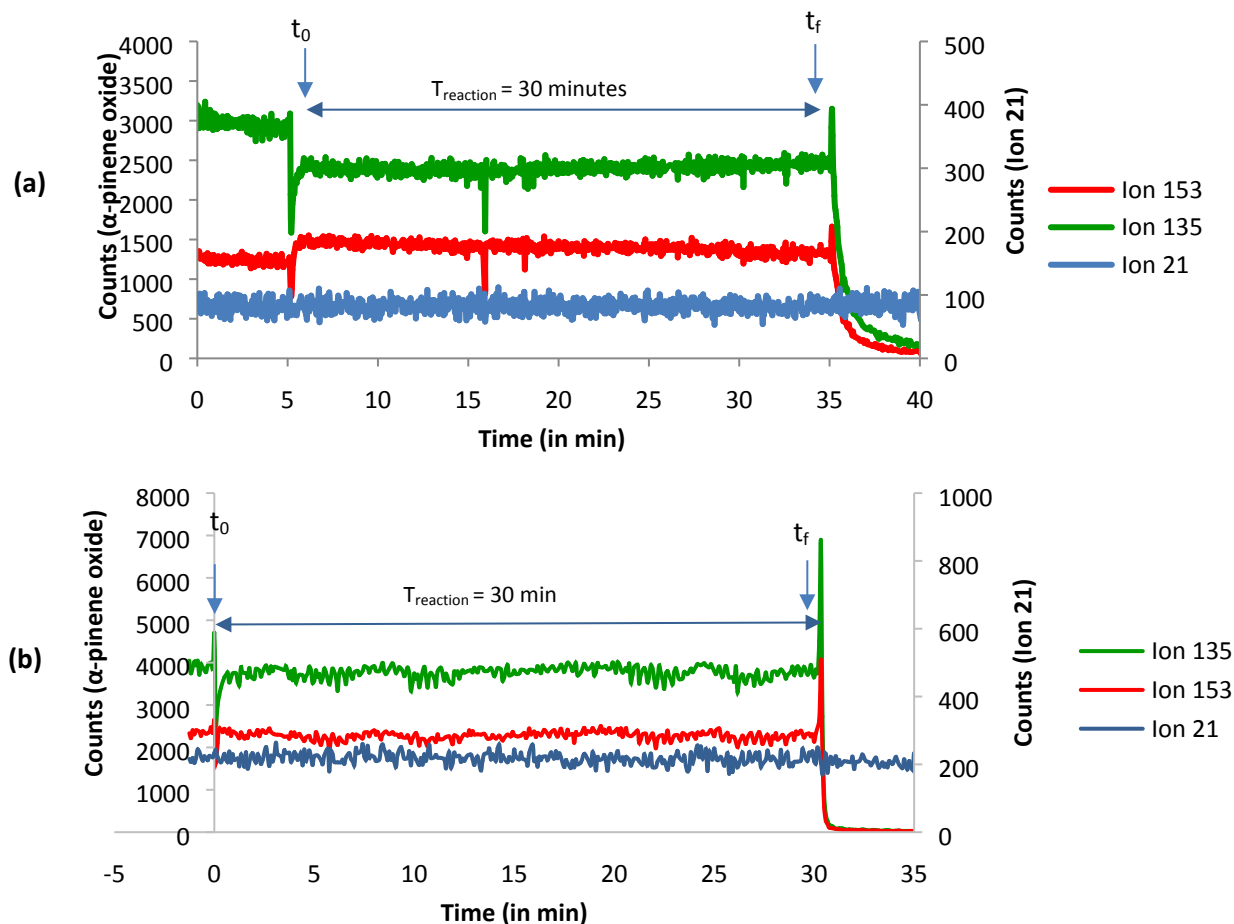


**Figure 1.** Typical evolution of  $m/z$  153,  $m/z$  135 and  $m/z$  21 ( $\text{H}_3^{18}\text{O}^+$ ) ions by PTR-TOF-MS during an experiment in quasi-static reactor between  $\alpha$ -pinene oxide (3.30 ppm) and ammonium sulfate aerosol under (a) highly acidic conditions and under (b) slightly acidic conditions –  $t_0$  is the time when the VOC flow was introduced in the reaction cell and  $t_f$  was the time when the VOC flow was stopped.

### Organosulfate formation

Overall, 132 experiments were performed in the present work to study the heterogeneous organosulfate formation from  $\alpha$ -pinene oxide under three different acidic conditions. Various  $\alpha$ -pinene oxide concentration levels (0.3-3.3 ppm) were tested for reaction times ranging from 0 to 400 min. As shown in the companion article,<sup>24</sup> more than 15 organosulfate (OS) products, including organosulfate dimers (DiOS) and trimers (TriOS) were formed from  $\alpha$ -pinene oxide under highly acidic conditions. The chromatograms and MS/MS fragmentation patterns allowing the identification of the organosulfates formed from  $\alpha$ -pinene oxide are fully described and discussed in light of previous studies in the companion article.<sup>24</sup> Table 3 summarizes the mass

1  
2  
3  
4  
5  
6  
7  
8  
9  
10  
11  
12  
13  
14  
15  
16  
17  
18  
19  
20  
21  
22  
23  
24  
25  
26  
27  
28  
29  
30  
31  
32  
33  
34  
35  
36  
37  
38  
39  
40  
41  
42  
43  
44  
45  
46  
47  
48  
49  
50  
51  
52  
53  
54  
55  
56  
57  
58  
59  
60

252 of organosulfates detected in these experiments. As an example, the OS masses detected in these experiments  
253 after 1 hour of reaction are also presented in Table 3.

254 In all conditions, the two main organosulfates  $m/z$  249 (i.e. OS 249 (1) and OS 249 (2)) have already been  
255 reported in some previous laboratory studies.<sup>22,23,48</sup> Note that these two compounds were not detected in a  
256 previous study in bulk aqueous solution by Bleier and Elrod (2013)<sup>38</sup> who detected a single organosulfate  
257 formed from the ring opening of  $\alpha$ -pinene oxide using  $^1\text{H}$  and  $^{13}\text{C}$  NMR characterization. Both OS 249 (1) and  
258 OS 249 (2) were also reported from various ambient aerosol analyses.<sup>14,22,46,47</sup> However, a very recent study  
259 based on the comparison of possible  $\alpha$ -hydroxy OS products formed from pinanediol and  $\alpha$ -pinene oxide to  
260 two regioisomers synthesized authentic standards evidenced that the compounds detected in a set of 18 ambient  
261 samples were not formed through  $\text{S}_\text{N}2$  reactions of  $\alpha$ -pinene oxide with  $\text{H}_2\text{O}$  or  $\text{H}_2\text{SO}_4$ <sup>49</sup> yielding to the  
262 conclusion that epoxides may not be the precursors of ambient bicyclic organosulfates.

263 In this work, the OS 249 monomers as well as the organosulfate dimers ( $m/z$  401, OS 401 and  $m/z$  481, OS  
264 481) were also detected under “slightly acidic” and “non-acidified” conditions, indicating that oligomerization  
265 processes do not require strong acidity conditions. Dehydration products of OS 249 ( $m/z$  231, MW 232) and  
266 OS 401 ( $m/z$  383, MW 384) were observed only under highly acidic conditions, indicating the key role of  
267  $\text{H}_2\text{SO}_4$  as both a strong acid and a strong hygroscopic reactant, on the dehydration of organosulfates and the  
268 formation of olefins in the atmosphere. Particle-phase dehydration of cyclic<sup>50</sup> and non-cyclic<sup>51</sup> hemiacetal  
269 compounds as well as organosulfates<sup>29</sup> was already observed to occur and lead to the formation of olefins in  
270 the presence of highly acidic or sulfuric acid particles. Consistently, this reaction was shown to be favored  
271 under low relative humidity conditions<sup>51</sup>. Hemiacetals or organosulfates dehydration products are unsaturated  
272 and hence more reactive towards atmospheric oxidants such as OH radicals,  $\text{NO}_3$  radicals, or  $\text{O}_3$ . Dehydration  
273 may thus affect in very specific (i.e. highly acidic and quasi-dry) conditions both the oxidation state and the  
274 reactivity of aerosols in the atmosphere. No organosulfate trimer was observed under slightly acidic conditions  
275 or with non-acidified ammonium sulfate aerosols. Table S1 presents the molecular structures proposed for the  
276 products identified in  $\alpha$ -pinene oxide experiments, performed under different aerosol acidities (Table 3).<sup>24</sup> The  
277 total organosulfate mass formed under highly acidic conditions was two orders of magnitude more abundant  
278 than those obtained under slightly acidic or neutral conditions. For the highly acidic aerosols, water may still

1  
2  
3 279 be present due to the highly hygroscopic nature of  $\text{H}_2\text{SO}_4$ <sup>52</sup> allowing  $\text{H}^+$  to drive the reaction. This emphasizes  
4  
5 280 the key role of  $\text{H}^+$  ions in organosulfate formation in the atmosphere. Nonetheless, organosulfate formation  
6  
7 281 did occur with non-acidified ammonium sulfate aerosols ( $(\text{NH}_4)_2\text{SO}_4$  at 0.06 M) showing that acidity from  
8  
9 282  $\text{NH}_4^+$  is sufficient to allow ring-opening of epoxide, in agreement with what was previously reported by  
10  
11 283 Nguyen et al.<sup>32</sup>

12  
13  
14 284  
15  
16

17 285 **Table 3. Organosulfate masses (in ng) quantified in quasi-static reactor experiments from  $\alpha$ -pinene oxide (3.3 ppm)**  
18 286 **using camphor sulfonic acid as an internal standard; HA : highly acidic particles, SA : slightly acidic particles, NA**  
19 287 **: non-acidified particles.**

Detected organosulfates	Highly acidic condition (HA) <sup>a</sup> (in ng) (R0)	Slightly acidic condition (SA) <sup>b</sup> (in ng) (R6)	Non-acidified condition (NA) <sup>c</sup> (in ng) (R10)
OS 231	0 – 1700 ( $190 \pm 60$ ) <sup>d</sup>	-	-
OS 249 (1)	0 – 50 480 ( $14\ 110 \pm 200$ ) <sup>d</sup>	0 – 740 (740) <sup>d</sup>	0 – 605 (511) <sup>d</sup>
OS 249 (2)	0 – 64 150 ( $8255 \pm 910$ ) <sup>d</sup>	0 – 1 430 (1430) <sup>d</sup>	0 – 570 (790) <sup>d</sup>
$\Sigma$ DiOS 401	0 – 26 660 ( $5350 \pm 1870$ ) <sup>d</sup>	0 – 200 (59) <sup>d</sup>	0 – 60 (24) <sup>d</sup>
$\Sigma$ DiOS 481	0 – 19 410 ( $3550 \pm 120$ ) <sup>d</sup>	0 – 20 (8) <sup>d</sup>	0 – 5 (2) <sup>d</sup>

20  
21  
22  
23  
24  
25  
26  
27  
28  
29 288  
30 289 <sup>a</sup> Reaction time: 0 – 400 min; <sup>b</sup> Reaction time: 0 – 90 min; <sup>c</sup> Reaction time: 0 – 60 min; <sup>d</sup> Mass of organosulfates detected after 60 min of reaction (for  
31 290 R0, n = 3; for R6 and R10, n = 1)

32 291 OS 249 (1) and OS 249 (2) were the two main organosulfates present at approximately the same  
33  
34 292 concentrations under highly acidic conditions, contrary to previous observations in chamber experiments by  
35  
36 293 Iinuma et al.<sup>23</sup>, where OS 249 (2) was the only main product. In their study, the authors suggested that the  
37  
38 294 dominance of the secondary carbon-substituted organosulfate indicates that sulfation reactions compete with  
39  
40 295 isomerization reactions leading to campholenic aldehyde and hence to a third  $m/z$  249 organosulfate, identified  
41  
42 296 as campholenol hydrogen sulfate (Figure S2). Previously, Liggio et al.<sup>29</sup> had also observed organosulfate  
43  
44 297 formation from the reactive uptake of pinonaldehyde on acidic sulfate particles and proposed a formation  
45  
46 298 mechanism via the protonation of the carbonyl group followed by the nucleophilic attack of  $\text{HSO}_4^-$ . Under our  
47  
48 299 experimental conditions and as discussed previously, campholenic aldehyde was highly suspected to be formed  
49  
50 300 in the gas phase (according to PTR-TOF-MS measurements). However, the continuous renewal of the gas  
51  
52 301 phase in the flow reactor cell may prevent from campholenic aldehyde accumulation in the flow reactor cell  
53  
54 302 and hence limit the occurrence of the gas-surface formation of a third  $m/z$  249 organosulfate which was not  
55  
56 303 detected in quasi-static reactor experiments. This is also in good agreement with the results reported by Iinuma  
57  
58  
59  
60

et al.<sup>23</sup> who have shown that the reaction yield of heterogeneous organosulfate formation from aldehydes may be low.

### Temporal profiles of organosulfate formation

Organosulfate temporal profiles are presented in the following section. These profiles were found to strongly depend on the particle acidity.

#### “Highly acidic” (HA) conditions

37 experiments (R0, Table 1) and 8 experiments (R1, Table 1) were carried out with 3.3 ppm and 1.0 ppm of  $\alpha$ -pinene oxide respectively, to describe the kinetics of organosulfate formation from  $\alpha$ -pinene oxide. Under highly acidic conditions, the concentrations increase linearly, with reaction time for all observed products, and may be described by the equation (1).

$$[OS] = k_{eff} \times t \quad (1)$$

As an example, Figure 1 presents the temporal profiles of OS 249 (2) organosulfate formation. The experimental data points were fitted using a linear regression ( $r^2 > 0.99$ ), showing that the reaction rate was constant over the reaction time. As presented previously, the concentration of  $\alpha$ -pinene oxide was constant under our experimental conditions. The first step of the organosulfate formation is supposed to be the protonation of the epoxide as presented in Figure S2. Thus, if this protonation is considered as the rate limiting step, a simple kinetic equation can be proposed in a first approach:

$$v = k' [APO] [H^+] = \frac{d[OS]}{dt} \quad (2)$$

with  $k'$  = the rate coefficient (in  $\text{cm}^3 \text{ molecule}^{-1} \text{ s}^{-1}$ ) of the protonation of  $\alpha$ -pinene oxide. As observed in the experiments, the OS formation rate shows that both reactants are in constant (stationary) concentrations under our experimental conditions, allowing Equation (2) to be reduced to (3):

$$\frac{d[OS]}{dt} = k_{eff} \quad (3)$$

With  $k_{eff} = k' [APO] [H]^+$  (in  $\text{molecule cm}^{-3} \text{ s}^{-1}$ )



From this kinetic behavior, as demonstrated by the linear plots of the reaction product formation shown in Figure 2a, it is assumed that  $H^+$  was also present in excess. More, the  $k_{\text{eff}}$  values are shown to vary linearly with  $\alpha$ -pinene oxide concentrations (Figure 2b). This result is well described by the kinetic equation presented previously, where  $k_{\text{eff}}$  is proportional to the  $\alpha$ -pinene oxide concentration under our experimental conditions. As it can be seen in Figure S3a, the effective rate coefficient determined for OS 249 (1) formed concomitantly to OS 249 (2) from the same set of experiments was found to vary between each of the 7 series of experiments performed with 3.3 ppm of  $\alpha$ -pinene oxide. Linear fit slopes varied daily from 0.13 to 0.34 ( $r^2 > 0.95$  for 6 series of experiments). During their preparation, particles were thoroughly dried prior to reaction allowing experiments to be carried out under quasi-dry conditions in the quasi-static reactor. Nonetheless, as explained previously, it cannot be excluded that the particle water content may have varied daily within the uncertainties of the balance used for the particle mass control (2-3 % of the particle mass). This small residual amount of water in the particles seems to have a critical role in OS 249 (1) formation pathway. Further investigation would be very useful to gain insight on this issue.

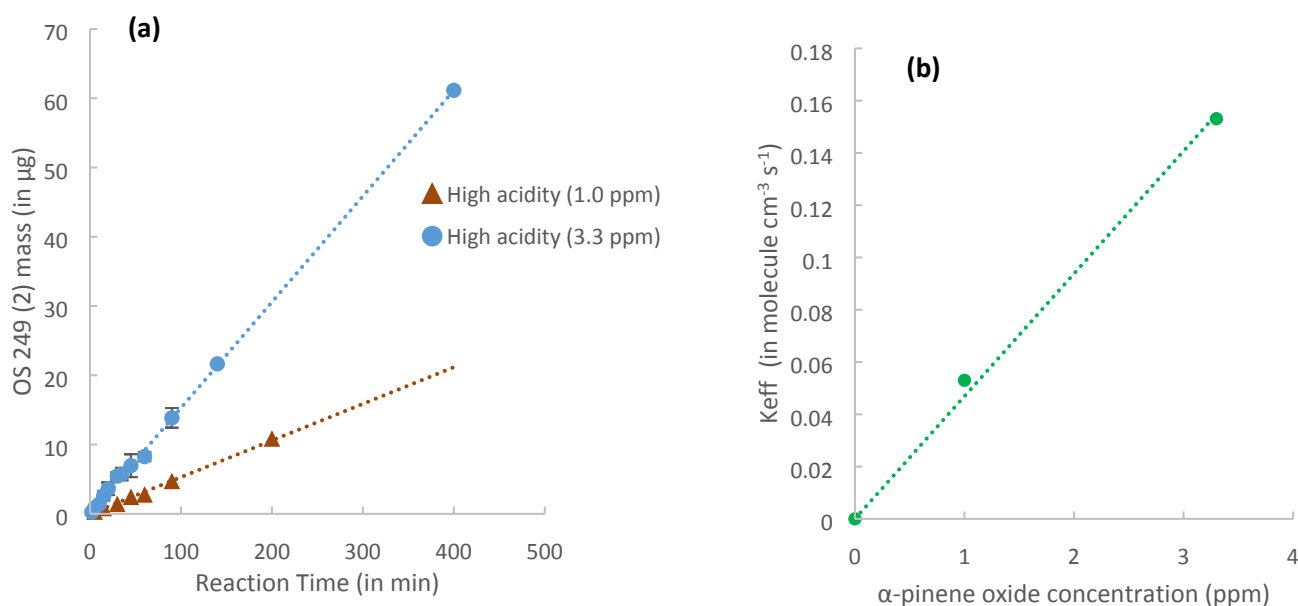
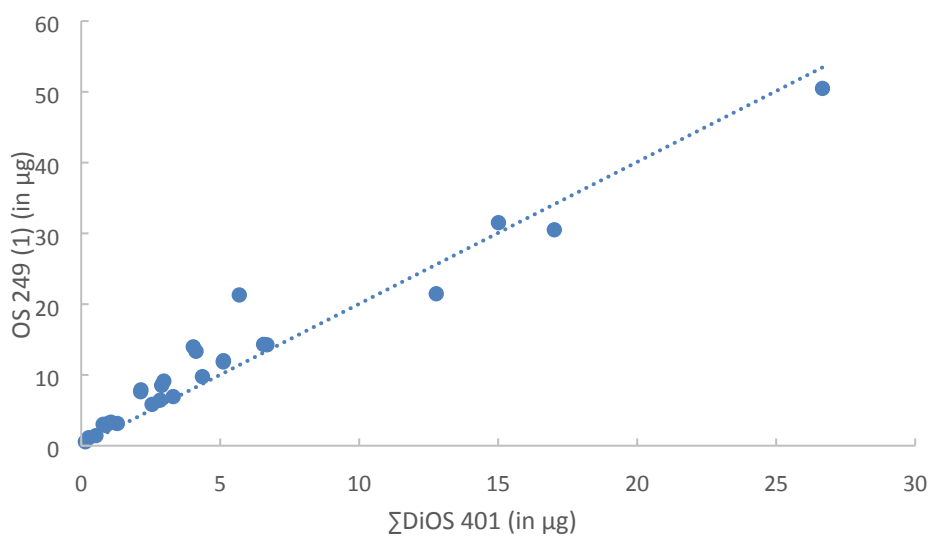


**Figure 2.** (a) Temporal profiles of  $m/z$  249 (2) organosulfate formation under highly acidic conditions, (b)  $k_{\text{eff}}$  values in function of  $\alpha$ -pinene oxide concentrations

1  
2  
3 352 The temporal profiles of  $m/z$  401 and  $m/z$  481 organosulfate dimers are shown in Figures S3c and S3d. First,  
4  
5 353 the oligomerization processes start very rapidly (within the first minutes of reaction) since organosulfate  
6  
7 354 dimers were detected in the particle phase after only 2 minutes of reaction. As presented in Figure 3, the  
8  
9 355 concentration of the sum of  $m/z$  401 organosulfate dimers is highly correlated to that of OS 249 (1) ( $r^2 = 0.92$ ).  
10  
11 356 In the proposed mechanism (see the companion article and Figure S2), the main  $m/z$  401 organosulfate (TR  
12  
13 357 21.3 min, representing from 65 to 80 % of the total concentration of  $\Sigma$ DiOS 401) is assumed to be formed via  
14  
15 358 the addition of OS 249 (2) on a tertiary carbocation intermediate (in the red dashed box, Figure S2), formed  
16  
17 359 from the protonation of  $\alpha$ -pinene oxide. This tertiary carbocation intermediate, also directly involved in the  
18  
19 360 formation of OS 249 (1), is assumed to be highly sensitive to the presence of water. Thus, the high correlation  
20  
21 361 between concentrations of OS 249 (1) and the sum of  $m/z$  401 organosulfate dimers from day to day (Figure  
22  
23 362 S3) firmly supports the proposed mechanism in the companion article.<sup>24</sup>



363  
364 **Figure 3.** Correlation between OS 249 (1) formation and  $\Sigma$ DiOS 401 formation from  $\alpha$ -pinene oxide under highly acidic  
365 conditions.

366  
367 Nonetheless, when  $\alpha$ -pinene oxide concentration was decreased from 3.3 ppm to 1.0 ppm, the effective reaction  
368 rate coefficients for OS 249 (1) and for  $\Sigma$ diOS 401 were estimated to be from (2.5 to 6.2) and (2.5 to 7.1) times  
369 lower, respectively. This suggests that the proposed kinetic model (as described in equation (2)) may also be  
370 valid for OS 249 (1) and diOS 401. Interestingly,  $m/z$  481 DiOS were formed in approximatively the same  
371 concentrations in experiments performed with 1.0 ppm and 3.3 ppm of  $\alpha$ -pinene oxide (Figure S3c), illustrating

1  
2  
3  
4  
5  
6  
7  
8  
9  
10  
11  
12  
13  
14  
15  
16  
17  
18  
19  
20  
21  
22  
23  
24  
25  
26  
27  
28  
29  
30  
31  
32  
33  
34  
35  
36  
37  
38  
39  
40  
41  
42  
43  
44  
45  
46  
47  
48  
49  
50  
51  
52  
53  
54  
55  
56  
57  
58  
59  
60

372 that the effective rate for the formation of these products does not depend on  $\alpha$ -pinene oxide concentration in  
373 the gaseous phase.

374 “Slightly acidic” (SA) and “non-acidified” (NA) conditions

375 In total, 71 experiments were carried out at various  $\alpha$ -pinene oxide concentrations: 3.30 ppm (n = 43), 1.65  
376 ppm (n = 13), 0.82 ppm (n = 10) and 0.33 ppm (n = 5) to gain further insights on the kinetics of organosulfate  
377 formation under slightly acidic conditions. As presented in Table 1, 16 experiments were also performed in  
378 this work in the presence of non-acidified ammonium sulfate aerosols. High variability of DiOS temporal  
379 profiles was observed due to levels near the detection limit and they are therefore not presented. Figure 4  
380 summarizes the temporal profiles of OS 249 (1) obtained under “slightly acidic” and “non-acidified”  
381 conditions. The experimental variability of the data points describing the OS 249 (1) formation is in agreement  
382 with the results presented above and may be tentatively explained as proposed by the variation of the residual  
383 amount of water in the particles. The experiments carried out with 3.3 ppm of  $\alpha$ -pinene oxide show that the  
384 formation of OS is limited under low acidity conditions, with a plateau reached ( $[\text{OS}]_{\text{max}} = 0.62 \mu\text{g}$ ) after  
385 around 15-20 minutes. The value of the plateau represents the OS maximum concentration formed under our  
386 experimental conditions. OS 249 (2) mass reached up to 1.4  $\mu\text{g}$  (Table 3), a plateau value higher than for OS  
387 249 (1) (contrary to the results obtained in highly acidic conditions), evidencing that acidity is a key parameter  
388 not only for global kinetics but also for the mechanistic pathways leading to organosulfate formation.

389 As OS formation was not limited with highly acidic particles, the plateau observed here with slightly acidic or  
390 non-acidified particles was not attributed to the presence of a very viscous organic phase or to phase-separated  
391 aerosols<sup>53</sup> but rather to the amount of protons available for reactions. A simple kinetics approach was proposed  
392 to model the formation of OS 249 (1): data points were fitted using a first order exponential function, defined  
393 as follows:

$$394 \quad [\text{OS}](t) = [\text{OS}]_{\text{max}} \times (1 - e^{-k't}) \quad (4)$$

395 where  $[\text{OS}](t)$  is the organosulfate concentration formed on the particles,  $[\text{OS}]_{\text{max}}$  the maximum organosulfate  
396 concentration and  $k'$  the pseudo-first order rate coefficient of the reaction. The fitting parameters are extracted  
397 from the Figure 4. Note that experiments performed at lower VOC concentrations could not be fitted using the

same parameter values, either because of the experimental variability of the data points or because the kinetic model is not appropriate. As a matter of fact, the plateau could also result from an equilibrium between organosulfate formation and reverse reaction or dimer formation. Further experiments will be needed to gain further insights on the kinetics of heterogeneous formation of organosulfate from  $\alpha$ -pinene oxide, especially as a function of aerosol surface area.

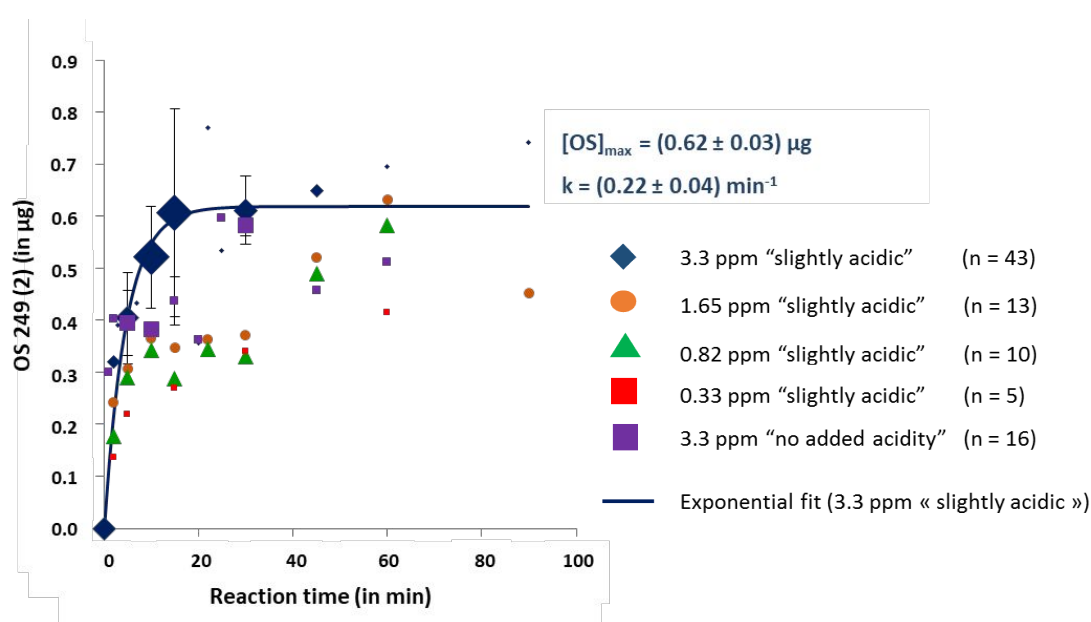


**Figure 4.** Temporal mass profiles of OS 249 (1) obtained in slightly acidic conditions and in the presence of sulfate ammonium aerosols - The size of data represents the number of experiments (ranging from 1 to 11)

Finally, the time profiles of organosulfate formation in "slightly acidic" or "no-added acidity" conditions were very similar, probably because of the low concentration of sulfuric acid in the "slightly acidic" conditions. This strongly suggests that in both conditions, the protonation of  $\alpha$ -pinene oxide to form the first intermediate occurs mostly via reaction with  $\text{NH}_4^+$ , in agreement with Nguyen et al.<sup>32</sup> It would be interesting to carry out further experiments by varying the amount of  $\text{NH}_4^+$  to firmly support the role of this ion.

In complement to these measurements in the quasi-static reactor, some experiments were carried out in atmospheric simulation chamber.

1  
2  
3  
4  
5  
6  
7  
8  
9  
10  
11  
12  
13  
14  
15  
16  
17  
18  
19  
20  
21  
22  
23  
24  
25  
26  
27  
28  
29  
30  
31  
32  
33  
34  
35  
36  
37  
38  
39  
40  
41  
42  
43  
44  
45  
46  
47  
48  
49  
50  
51  
52  
53  
54  
55  
56  
57  
58  
59  
60

## 423 **Organosulfate formation from $\alpha$ -pinene oxide – chamber experiments**

### 424 **Gas phase**

425 Depending on experimental conditions, a decrease of about 10 to 50 % of  $\alpha$ -pinene oxide concentration in 60  
426 minutes was measured in the CESAM chamber, with or without particles. This unusually fast wall loss (even  
427 for an oxygenated compound) was attributed to isomerization processes on the metallic wall surface. PTR-  
428 TOF-MS data measurements displayed a decrease of the  $m/z$  135 fragment signal as well as an increase at  $m/z$   
429 153. Thus, formation of campholenic aldehyde or other isomerization products of  $\alpha$ -pinene oxide were  
430 assumed to occur in CESAM. Previous studies have reported the isomerization of  $\alpha$ -pinene oxide using Fe-  
431 supported catalysts<sup>54</sup> and CESAM stainless steel wall might play a role in this particular reaction. However,  
432  $\alpha$ -pinene oxide was found to be stable in CESAM chamber under humid conditions (RH = 20 % and RH = 50  
433 %) <sup>24</sup>, highlighting that the  $\alpha$ -pinene oxide loss was influenced by the presence of condensable species such as  
434 water. Note that cyclohexene oxide (Sigma Aldrich, 98 %) was found to be stable in the CESAM chamber,  
435 showing that wall loss was specific to  $\alpha$ -pinene oxide, corroborating that this loss was likely due to  
436 isomerization. It is worth noting that the  $\alpha$ -pinene oxide loss to the CESAM chamber walls cannot be explained  
437 by memory effects from prior experiments conducted in the presence of acidic sulfate aerosol because the  
438 chamber walls were manually cleaned with purified water and ethanol and by maintaining a secondary vacuum  
439 ( $\sim 6 \times 10^{-4}$  hPa) overnight.

440 The amount of  $\alpha$ -pinene oxide which reacted on particles was roughly inferred from the total amount of  
441 organosulfate formed in the chamber. From this calculation and the concentration of  $\alpha$ -pinene oxide measured  
442 in the gas-phase, it could be estimated that about 0.05 % of the initial gaseous  $\alpha$ -pinene oxide had reacted on  
443 particles. It was thus considered that regardless of the wall loss, gaseous  $\alpha$ -pinene oxide was present in a large  
444 excess during the experiments in CESAM and hence that OS formation occurred under pseudo-first order  
445 conditions.

### 446 **Organosulfate formation**

447 Figure 5a summarizes organosulfate concentrations (in  $\text{ng m}^{-3}$ ) measured in the aerosol phase obtained in  
448 CESAM when  $\alpha$ -pinene oxide was introduced in the presence of sulfated aerosols. No clear increase of the  
449 particle mass concentration was observed in the experiments with an initial seed aerosol mass of about 20  $\mu\text{g}$

1  
2  
3 450  $\text{m}^{-3}$ , regardless of the aerosol acidity conditions (experiments C1, C7 and C8). Considering the wide size  
4  
5 451 distribution of the seed particles in these 3 experiments, the uncertainty associated to the measurements of  
6  
7 452 particle mass concentration using SMPS (about  $1 \mu\text{g m}^{-3}$ ) hindered to detect any aerosol mass growth related  
8  
9 453 to organosulfate formation (Figure 5a). However, in experiment C4, the aqueous solution containing the seed  
10  
11 454 aerosol constituents was diluted by a factor 10, resulting in the introduction of smaller particles in the chamber.  
12  
13 455 Under these specific experimental conditions, a clear increase of about  $3 \mu\text{g m}^{-3}$  in the particle mass  
14  
15 456 concentration was observed (Figure S4) along the experiment, suggesting that  $\alpha$ -pinene oxide may be an  
16  
17 457 effective organosulfate precursor especially in region area dominated by trees which largely emit  
18  
19 458 monoterpenes. It is worth noting that OS 249 have been observed in many regions of the world<sup>14,15,22,23,46</sup>,  
20  
21 459 suggesting that OS formation from  $\alpha$ -pinene oxide occurs under ambient conditions, although their exact  
22  
23 460 structures were recently discussed<sup>49</sup>.  
24  
25  
26  
27 461  
28  
29  
30  
31  
32  
33  
34  
35  
36  
37  
38  
39  
40  
41  
42  
43  
44  
45  
46  
47  
48  
49  
50  
51  
52  
53  
54  
55  
56  
57  
58  
59  
60

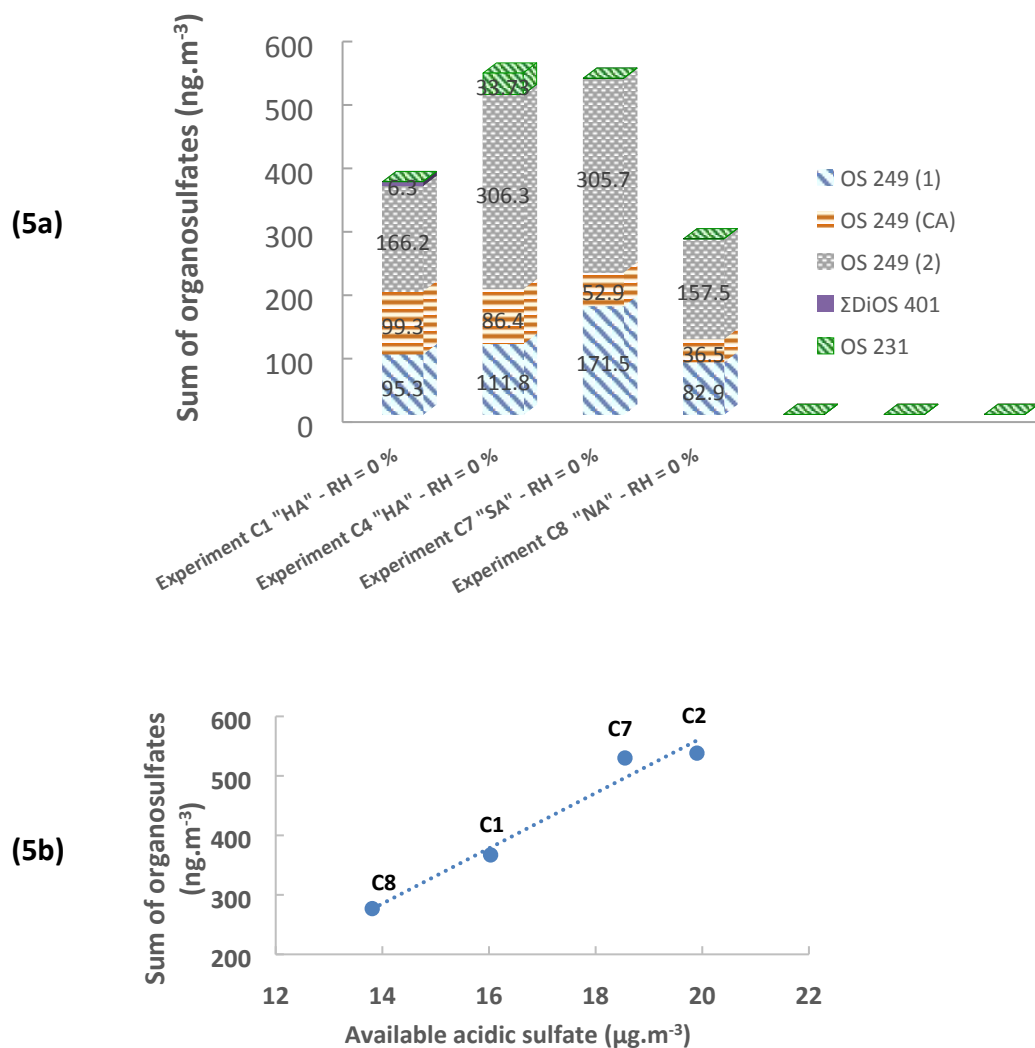


**Figure 5.** (a) Sum of organosulfates and (b) organosulfate mass concentrations as a function of the available acidic sulfate concentration in the particle phase for  $\alpha$ -pinene oxide experiments in the CESAM chamber

Interestingly, organosulfate concentrations are of the same order of magnitude in all experiments performed without water vapor injection, independently of the presence of acidified sulfate aerosols (Figure 5a), contrary to the results obtained from quasi-static reactor experiments or in previous works.<sup>6,39</sup> As previously shown for monoterpene oxides in chamber<sup>23</sup> and bulk solution<sup>34</sup> experiments, formation yields of organosulfates were shown to depend on the available sulfate concentration. In agreement with these studies, Figure 5b displays the relationship between the total OS concentration and the sulfate aerosol concentration, highlighting the importance of the available surface area in heterogeneous reactions. Further investigation involving total aerosol surface area and condensation sink did not allow us to provide a straightforward relationship with OS formation amounts.

1  
2  
3 481 It is also worth noting that the concentration of OS 249 (CA) from campholenic aldehyde was increased when  
4  
5 482 increasing the particle acidity. As reported in Figure 5a, the concentration of this organosulfate ( $99 \text{ ng m}^{-3}$  for  
6  
7 483 C1 and  $86.4 \text{ ng m}^{-3}$  for C4) is more important under highly acidic conditions than under slightly ( $53 \text{ ng m}^{-3}$  for  
8  
9 484 C7) or non-acidified ones ( $37 \text{ ng m}^{-3}$ ), suggesting that  $\alpha$ -pinene oxide isomerization is favored under acidic  
10  
11 485 conditions. Moreover, the OS 249 (1)/OS 249 (CA) concentration ratio was decreased with increasing acidity  
12  
13 486 (HA: 1.0 (C1) and 0.8 (C4); SA: 0.3 (C7); NA: 0.4 (C8)), suggesting the competition for the tertiary  
14  
15 487 carbocation intermediate between isomerization and  $\text{HSO}_4^-$  attack, as proposed in the formation mechanism  
16  
17 (Figure S2). An example of temporal profiles of organosulfate formation in CESAM is presented in Figure S5.  
18 488  
19  
20 489 In the 4 experiments, organosulfates were formed rapidly in the first few minutes and reached a threshold value  
21  
22 490 independently of the particle acidity, suggesting that the available aerosol surface area is a key parameter in  
23  
24 491 these heterogeneous processes. Temporal variations were similar for all other experiments, showing no effects  
25  
26 492 of acidity on the dynamics of organosulfate formation under these experimental conditions.  
27  
28  
29 493

### 31 494 **Organosulfate formation from other precursors - comparison of temporal variations**

32  
33 495 As shown in the companion article, organosulfates are also formed from other precursors. Their formation  
34  
35 496 kinetics was studied, as for  $\alpha$ -pinene oxide, under pseudo-first order conditions. During all experiments, the  
36  
37 497 gas concentration of each VOC was checked to be constant in the reaction cell by on-line monitoring using  
38  
39 498 PTR-TOF-MS. Their temporal profiles derived from quasi-static reactor experiments are presented and  
40  
41 499 discussed below.  
42  
43  
44

#### 45 500 **Organosulfates $m/z$ 249**

46  
47 501 Figure 6 presents the temporal mass variations of OS 249 (1) and OS 249 (2), the two main products formed  
48  
49 502 from experiments between highly acidic sulfate aerosols and  $\alpha$ -pinene oxide, pinanediol or myrtenal ( $[\text{VOC}]$   
50  
51 503 =  $1.0 \text{ ppm}$ ). Similarly, to the case of  $\alpha$ -pinene oxide reaction, experimental data points issued from pinanediol  
52  
53 504 and myrtenal could be nicely fitted with a linear regression. Although such temporal profiles only provide  
54  
55 505 preliminary information on organosulfate formation kinetics, it is relevant to compare in a first approach the  
56  
57 506 slopes of the linear fits to determine organosulfate formation rates. The apparent rate coefficient  $k_{\text{eff}}(\alpha\text{-pinene}$   
58  
59 507 oxide) is 11 and 23 times larger than  $k_{\text{eff}}(\text{myrtenal})$  and  $k_{\text{eff}}(\text{pinanediol})$  for OS 249 (1), respectively. Similarly,



1  
2  
3  
4  
5  
6  
7  
8  
9  
10  
11  
12  
13  
14  
15  
16  
17  
18  
19  
20  
21  
22  
23  
24  
25  
26  
27  
28  
29  
30  
31  
32  
33  
34  
35  
36  
37  
38  
39  
40  
41  
42  
43  
44  
45  
46  
47  
48  
49  
50  
51  
52  
53  
54  
55  
56  
57  
58  
59  
60

508  $k_{\text{eff}}(\alpha\text{-pinene oxide})$  is 14 times higher than  $k_{\text{eff}}(\text{pinanediol})$  for OS 249 (2). Note that the formation of OS 249  
(2) was very limited for myrtenal with respect to OS 249 (1). This study provides quantitative results showing  
that epoxides are favored reactants to form organosulfates via heterogeneous gas-particle reactions, in  
agreement with previous studies.<sup>24,34,36,55</sup>

512

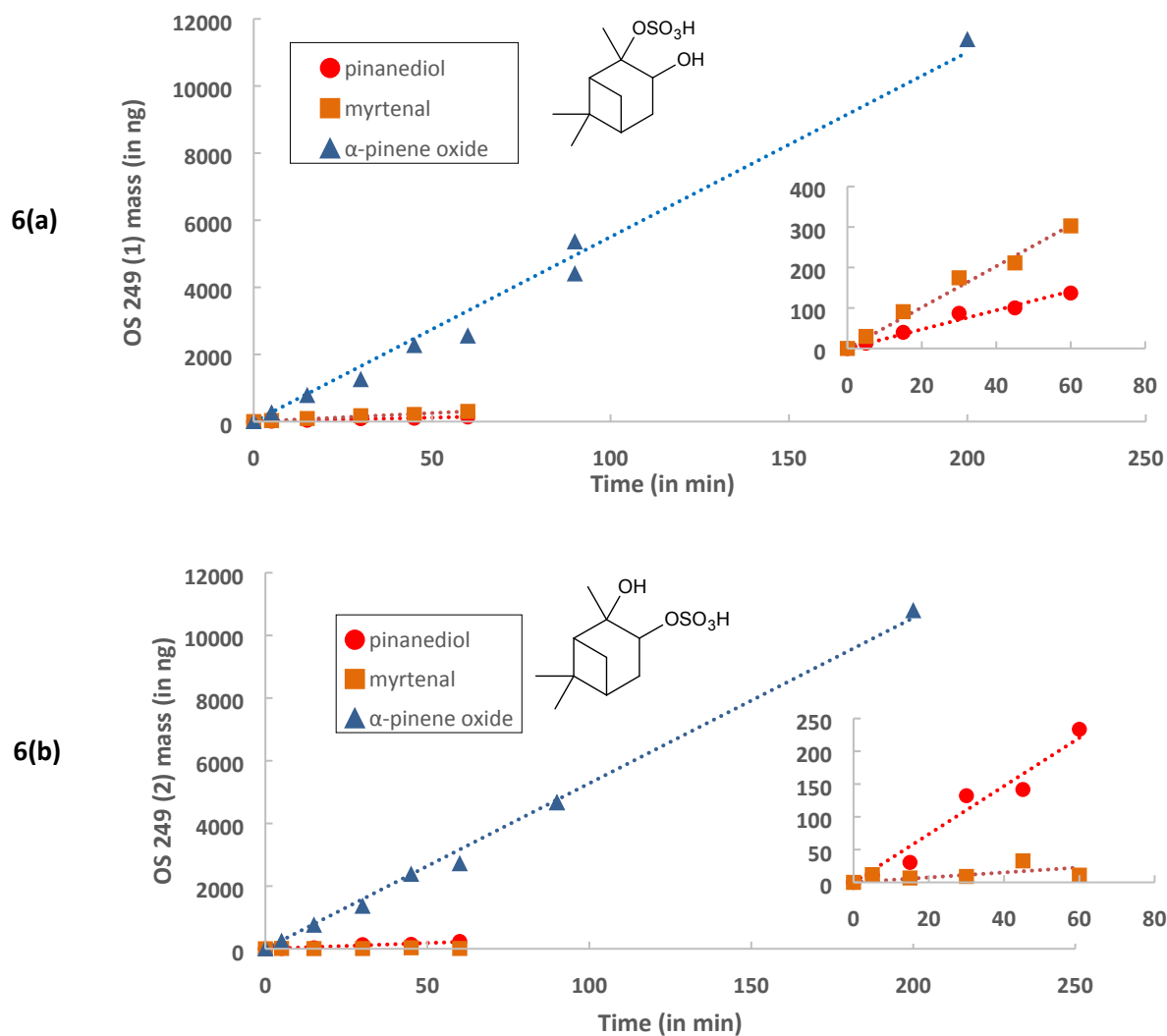


**Figure 6.** Temporal mass variations of OS 249 (1) (6a) and OS 249 (2) (6b) from reactions between acidified ammonium sulfate particles  $(\text{NH}_4)_2\text{SO}_4/\text{H}_2\text{SO}_4$  (0.03/0.05 M) and  $\alpha$ -pinene oxide, myrtenal or pinanediol (1.0 ppm)

### Organosulfates $m/z$ 233

The organosulfate  $m/z$  233 formation pathways from  $\alpha$ -pinene and isopinocampheol were already presented in the companion article.<sup>24</sup> Figure 7 presents the temporal mass variations of the two main  $m/z$  233 organosulfates formed from  $\alpha$ -pinene and isopinocampheol reactions under highly acidic conditions. Contrary to the  $m/z$  249 organosulfates, the kinetic models for OS 233 (1) and OS 233 (2) formations appear different according to the studied precursor. Experimental data points from isopinocampheol experiments could also be fitted using a linear regression. The values of  $k_{\text{eff}}$  are of the same order of magnitude than  $k_{\text{eff}}(\text{pinanediol})$  or  $k_{\text{eff}}(\text{myrtenal})$  for both organosulfates. This was not the case for the reaction with  $\alpha$ -pinene, where a plateau was reached for both OS 233 after about 15 min.

1

2

3 527 Experimental data points were fitted using a first order exponential function to provide a first quantitative  
 4  
 5 528 insight into this reaction. The results highlight here two different formation behaviors, in agreement with the  
 6  
 7 529 proposed mechanism (see the companion article).<sup>24</sup> The sulfation of  $\alpha$ -pinene occurs via the addition of sulfate  
 8  
 9 530 on the C-C double bond whereas the sulfation of isopinocampheol occurs via the nucleophilic substitution of  
 10  
 11 531 the hydroxyl functional group by the bisulfate anion. Therefore, in the first case, the initial step is the addition  
 12  
 13  
 14 532 of a proton on the C-C double bond whereas it is a nucleophilic attack of the leaving group, for  
 15  
 16 533 isopinocampheol reaction. Finally, temporal mass variations of OS 233 (3) from isopinocampheol is proposed  
 17  
 18 534 in Figure S6. This compound was formed in the first few minutes and seemed to decrease afterwards but no  
 19  
 20 535 clear trend was evidenced in its formation. Since this compound was not positively identified, further  
 21  
 22 536 information on its formation pathway cannot be proposed.

23

24

25 537

26

27

28

29

30

31

32

33

34

35

36

37

38

39

40

41

42

43

44

45

46

47

48

49

50

51

52

53

54

55

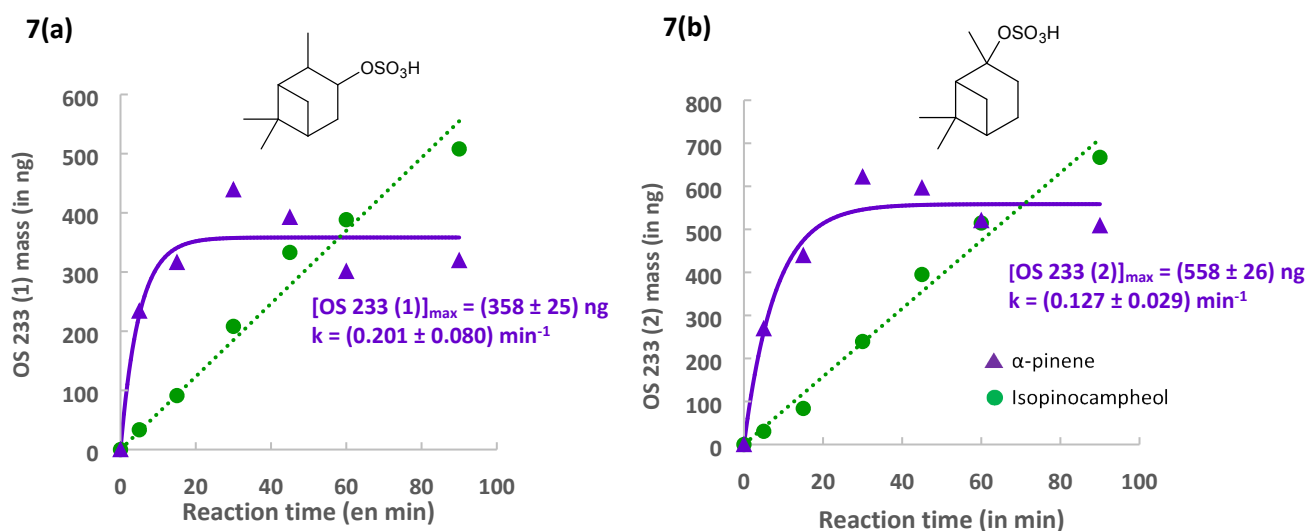
56

57

58

59

60



41 538

42

43 539

44 540

45

46 541

47

48 542

49

50

51 543

52

53 544

54

55 545

56

57 546

58

59 547

60

## 542 Conclusion

543 In the present study,  $\alpha$ -pinene oxide has been identified as the most efficient precursor of  $\alpha$ -pinene-derived  
 544 organosulfates observed in field studies.<sup>14,22,23,28,45</sup> The amount of organosulfates formed in quasi-static reactor  
 545 experiments was found to increase notably with higher aerosol acidity. It was also found that the mass  
 546 concentrations of organosulfates depend on the available sulfate in the aerosol phase in chamber experiments,  
 547 in agreement with previous studies.<sup>23,55</sup> In this work, the oligomerization processes was observed under both

1  
2  
3 548 low and high acidic conditions. This suggests that the formation of organosulfate dimers from  $\alpha$ -pinene oxide  
4  
5 549 may contribute to SOA composition in the atmosphere on a large aerosol pH range and more specifically where  
6  
7 550 highly acidic aerosols ( $\text{pH} < 1$ ) have been reported.<sup>56-58</sup>. These results also provide some new organosulfate  
8  
9 551 structures to be looked for in field studies, especially in environments where monoterpenes are the predominant  
10  
11 552 BVOCs.

13  
14 553 This study also presents an extensive laboratory investigation of organosulfate formation from oxidation  
15  
16 554 products of  $\alpha$ -pinene or proxies, with ammonium sulfate model aerosols. Temporal variations of organosulfate  
17  
18 555 concentrations, for the reactions of  $\alpha$ -pinene,  $\alpha$ -pinene oxide, isopinocampheol, pinanediol and myrtenal are  
19  
20 556 presented and discussed for the first time. For all precursors, except for  $\alpha$ -pinene under highly acidic  
21  
22 557 conditions, organosulfate formation was found to be linear with reaction time, showing that all reactants were  
23  
24 558 present in a large excess. Effective rate coefficients for OS formation were determined to be one or two orders  
25  
26 559 of magnitude higher for  $\alpha$ -pinene oxide than for the 4 other precursors. Although some recent studies<sup>38,49</sup> still  
27  
28 560 question the exact OS carbon backbone structures and formation mechanisms highlighting the need of further  
29  
30 561 investigations, this work allows to conclude that epoxides appears as a favored reactant to form organosulfates  
31  
32 562 via heterogeneous gas-particle reactions under our experimental conditions.

33  
34  
35  
36 563 As a future work, it would be interesting to use this methodology to compare the apparent rate coefficient of  
37  
38 564 OS formation from IEPOX and  $\alpha$ -pinene oxide, and then assess their contribution to OS formation under  
39  
40 565 similar conditions. In the presence of slightly acidic or non-acidified ammonium sulfate aerosols, the amounts  
41  
42 566 of organosulfates were much lower than those obtained under highly acidic conditions, showing that  
43  
44 567 ammonium ions may be involved in OS formation via a slightly different mechanism, also depending on the  
45  
46 568 aerosol acidity and the RH/aerosol water content. The complementary study in CESAM chamber have shown  
47  
48 569 the OS formation under more realistic conditions and have given first kinetic description of the studied  
49  
50 570 mechanistic pathways. The experiments performed in the CESAM chamber were designed to allow us to  
51  
52 571 confront the mechanistic and kinetic results on OS formation obtained in a quasi-static reactor to experimental  
53  
54 572 data determined for specific and selected chemical systems in more realistic conditions (e.g. using suspended  
55  
56 573 aerosol instead of deposited on a filter). Hence, both experimental approaches were highly complementary and  
57  
58 574 fruitfully associated in this work. Although the present study provides highly robust and relevant new  
59  
60

1  
2  
3 575 knowledge on heterogeneous OS formation, the kinetic data are yet “experimental condition”-dependent and  
4  
5 576 thus cannot be directly implemented in an atmospheric chemistry box-model to evaluate the contribution of  $\alpha$ -  
6  
7 577 pinene oxide to OS formation in the atmosphere. Therefore, further experiments more specifically focused on  
8  
9 578 OS formation from  $\alpha$ -pinene oxide are needed to extend our experimental approach relying in the fruitful  
10  
11 579 association of quasi-static reactor and atmospheric simulation chamber to a wider range of experimental  
12  
13 580 conditions (i.e.  $\alpha$ -pinene oxide concentrations, RH, acidity and sulfate concentration...). This should then  
14  
15 581 achieve the complete kinetic parametrization of this complex gas-surface reaction and allow the  
16  
17 582 implementation of OS heterogeneous formation in atmospheric chemical models. Nevertheless, this study  
18  
19 583 already illustrates how gas-particle reactions may play an important role in OS formation and hence in the  
20  
21 584 atmospheric fate of organic carbon.<sup>53,59</sup>  
22  
23  
24  
25 585

## 27 586 ASSOCIATED CONTENT

### 30 587 **Supporting Information.**

32  
33 588 Figure S1 presents the mass spectra from PTR-TOF-MS for  $\alpha$ -pinene oxide and campholenic  
34  
35 589 aldehyde. Figure S2 displays the proposed organosulfate formation mechanism from  $\alpha$ -pinene oxide.  
36  
37 590 Figure S3 presents the temporal mass profiles of  $m/z$  249 (1),  $m/z$  401 and  $m/z$  481 organosulfate  
38  
39 591 formation in the particulate phase. Figure S4 shows the aerosol particle concentration in the CESAM  
40  
41 592 chamber measured during the C4 experiment. Figure S5 presents the temporal variations of OS 249  
42  
43 593 (1), OS 249 (2) and OS 249 (CA) from  $\alpha$ -pinene oxide under non-acidified sulfate conditions in the  
44  
45 594 CESAM chamber. Figure S6 presents the temporal mass profile of OS 233 (3) from experiments  
46  
47 595 between acidic sulfated aerosols  $(\text{NH}_4)_2\text{SO}_4/\text{H}_2\text{SO}_4$  (0.03/0.05 M) and isopinocampheol. Table S1  
48  
49 596 shows the structure of the organosulfates detected in  $\alpha$ -pinene oxide experiments. The Supporting  
50  
51 597 Information is available free of charge on the ACS Publications website <http://pubs.acs.org>.  
52  
53  
54  
55  
56  
57 598  
58  
59  
60

1  
2  
3 599 AUTHOR INFORMATION  
45 600 **Corresponding Author**  
67 601 \*Emilie Perraudin. E-mail address: emilie.perraudin@u-bordeaux.fr  
8  
910 602 **Notes**  
1112 603 The authors declare no competing financial interest.  
1314 604 This study was part of the PhD work defended by Geoffroy Duporté at the University of Bordeaux,  
15 605 France, the 1<sup>st</sup> December 2014 and entitled “Formation et devenir de l’aérosol organique secondaire  
16 606 : étude expérimentale de formation d’organosulfates à l’interface gaz-particules”.  
17  
18  
1920 607 **Acknowledgments**  
21  
2223 608 The authors wish to thank the CNRS-INSU LEFE-CHAT program, the Aquitaine Region, the University of  
24 609 Bordeaux and the French National Agency for Research (ANR) through the COGNAC project (n° ANR-13-  
25 610 BS06-0002-03) for financial support. CNRS-INSU is also acknowledged for supporting the CESAM chamber  
26 611 as a national instrument. This work was also supported by the European Commission through  
27 612 EUROCHAMP-2 (contract no. 228335). The authors are also deeply grateful to Prof. Jason Surratt from  
28 613 UNC for very helpful discussions and for kind and careful proofreading of this manuscript. Finally, the authors  
29 614 wish to gratefully acknowledge the JPC A reviewers for their valuable comments.  
30  
31  
32  
33  
34  
35  
36  
37  
38  
39  
40  
41  
42  
43  
44  
45  
46  
47  
48  
49  
50  
51  
52  
53  
54  
55  
56  
57  
58  
59  
60

1  
2  
3  
4  
5  
6  
7  
8  
9  
10  
11  
12  
13  
14  
15  
16  
17  
18  
19  
20  
21  
22  
23  
24  
25  
26  
27  
28  
29  
30  
31  
32  
33  
34  
35  
36  
37  
38  
39  
40  
41  
42  
43  
44  
45  
46  
47  
48  
49  
50  
51  
52  
53  
54  
55  
56  
57  
58  
59  
60**References**

- (1) Pope III, C. A.; Dockery, D. W. Health Effects of Fine Particulate Air Pollution: Lines That Connect. *Journal of the air & waste management association* **2006**, *56* (6), 709–742.
- (2) Kanakidou, M.; Seinfeld, J. H.; Pandis, S. N.; Barnes, I.; Dentener, F. J.; Facchini, M. C.; Dingenen, R. V.; Ervens, B.; Nenes, A.; Nielsen, C. J. Organic Aerosol and Global Climate Modelling: A Review. *Atmospheric Chemistry and Physics* **2005**, *5* (4), 1053–1123.
- (3) Stocker, T. *Climate Change 2013: The Physical Science Basis: Working Group I Contribution to the Fifth Assessment Report of the Intergovernmental Panel on Climate Change*; Cambridge University Press, 2014.
- (4) Hallquist, M.; Wenger, J. C.; Baltensperger, U.; Rudich, Y.; Simpson, D.; Claeys, M.; Dommen, J.; Donahue, N. M.; George, C.; Goldstein, A. H. The Formation, Properties and Impact of Secondary Organic Aerosol: Current and Emerging Issues. *Atmospheric chemistry and physics* **2009**, *9* (14), 5155–5236.
- (5) Nozière, B.; Kalberer, M.; Claeys, M.; Allan, J.; D’Anna, B.; Decesari, S.; Finessi, E.; Glasius, M.; Grgić, I.; Hamilton, J. F.; et al. The Molecular Identification of Organic Compounds in the Atmosphere: State of the Art and Challenges. *Chem. Rev.* **2015**, *115* (10), 3919–3983. <https://doi.org/10.1021/cr5003485>.
- (6) Surratt, J. D.; Kroll, J. H.; Kleindienst, T. E.; Edney, E. O.; Claeys, M.; Sorooshian, A.; Ng, N. L.; Offenberg, J. H.; Lewandowski, M.; Jaoui, M. Evidence for Organosulfates in Secondary Organic Aerosol. *Environmental Science & Technology* **2007**, *41* (2), 517–527.
- (7) Iinuma, Y.; Müller, C.; Berndt, T.; Böge, O.; Claeys, M.; Herrmann, H. Evidence for the Existence of Organosulfates from  $\beta$ -Pinene Ozonolysis in Ambient Secondary Organic Aerosol. *Environmental Science & Technology* **2007**, *41* (19), 6678–6683.
- (8) Riva, M.; Tomaz, S.; Cui, T.; Lin, Y.-H.; Perraudin, E.; Gold, A.; Stone, E. A.; Villenave, E.; Surratt, J. D. Evidence for an Unrecognized Secondary Anthropogenic Source of Organosulfates and Sulfonates: Gas-Phase Oxidation of Polycyclic Aromatic Hydrocarbons in the Presence of Sulfate Aerosol. *Environmental science & technology* **2015**, *49* (11), 6654–6664.
- (9) Gómez-González, Y.; Surratt, J. D.; Cuyckens, F.; Szmigielski, R.; Vermeylen, R.; Jaoui, M.; Lewandowski, M.; Offenberg, J. H.; Kleindienst, T. E.; Edney, E. O. Characterization of Organosulfates from the Photooxidation of Isoprene and Unsaturated Fatty Acids in Ambient Aerosol Using Liquid Chromatography/(-) Electrospray Ionization Mass Spectrometry. *Journal of Mass Spectrometry* **2008**, *43* (3), 371–382.
- (10) Altieri, K. E.; Turpin, B. J.; Seitzinger, S. P. Oligomers, Organosulfates, and Nitrooxy Organosulfates in Rainwater Identified by Ultra-High Resolution Electrospray Ionization FT-ICR Mass Spectrometry. *Atmospheric Chemistry and Physics* **2009**, *9* (7), 2533–2542.
- (11) Hatch, L. E.; Creamean, J. M.; Ault, A. P.; Surratt, J. D.; Chan, M. N.; Seinfeld, J. H.; Edgerton, E. S.; Su, Y.; Prather, K. A. Measurements of Isoprene-Derived Organosulfates in Ambient Aerosols by Aerosol Time-of-Flight Mass Spectrometry-Part 1: Single Particle Atmospheric Observations in Atlanta. *Environmental science & technology* **2011**, *45* (12), 5105–5111.
- (12) Hatch, L. E.; Creamean, J. M.; Ault, A. P.; Surratt, J. D.; Chan, M. N.; Seinfeld, J. H.; Edgerton, E. S.; Su, Y.; Prather, K. A. Measurements of Isoprene-Derived Organosulfates in Ambient Aerosols by Aerosol Time-of-Flight Mass Spectrometry Part 2: Temporal Variability and Formation Mechanisms. *Environmental science & technology* **2011**, *45* (20), 8648–8655.
- (13) Stone, E. A.; Yang, L.; Yu, L. E.; Rupakheti, M. Characterization of Organosulfates in Atmospheric Aerosols at Four Asian Locations. *Atmospheric Environment* **2012**, *47*, 323–329. <https://doi.org/10.1016/j.atmosenv.2011.10.058>.
- (14) Ma, Y.; Xu, X.; Song, W.; Geng, F.; Wang, L. Seasonal and Diurnal Variations of Particulate Organosulfates in Urban Shanghai, China. *Atmospheric environment* **2014**, *85*, 152–160.
- (15) Hansen, A. M. K.; Kristensen, K.; Nguyen, Q. T.; Zare, A.; Cozzi, F.; Nøjgaard, J. K.; Skov, H.; Brandt, J.; Christensen, J. H.; Ström, J. Organosulfates and Organic Acids in Arctic Aerosols: Speciation, Annual Variation and Concentration Levels. *Atmospheric Chemistry and Physics* **2014**, *14* (15), 7807–7823.

1

2

- 3 673 (16) Brüggemann, M.; Poulain, L.; Held, A.; Stelzer, T.; Zuth, C.; Richters, S.; Mutzel, A.; van Pinxteren, D.;  
4 674 Iinuma, Y.; Katkevica, S.; et al. Real-Time Detection of Highly Oxidized Organosulfates and BSOA  
5 675 Marker Compounds during the F-BEACH 2014 Field Study. *Atmospheric Chemistry and Physics* **2017**,  
6 676 *17* (2), 1453–1469. <https://doi.org/10.5194/acp-17-1453-2017>.
- 7 677 (17) Barbosa, T. S.; Riva, M.; Chen, Y.; da Silva, C. M.; Ameida, J. C. S.; Zhang, Z.; Gold, A.; Arbilla, G.;  
8 678 Bauerfeldt, G. F.; Surratt, J. D. Chemical Characterization of Organosulfates from the Hydroxyl Radical-  
9 679 Initiated Oxidation and Ozonolysis of Cis-3-Hexen-1-ol. *Atmospheric Environment* **2017**, *162*, 141–151.  
10 680 <https://doi.org/10.1016/j.atmosenv.2017.04.026>.
- 11 681 (18) Le Breton, M.; Wang, Y.; Hallquist, A. M.; Kant Pathak, R.; Zheng, J.; Yang, Y.; Shang, D.; Glasius, M.;  
12 682 Bannan, T. J.; Liu, Q.; et al. Online Gas- and Particle-Phase Measurements of Organosulfates,  
13 683 Organosulfonates and Nitrooxy Organosulfates in Beijing Utilizing a FIGAERO ToF-CIMS. *Atmospheric*  
14 684 *Chemistry and Physics* **2018**, *18* (14), 10355–10371. <https://doi.org/10.5194/acp-18-10355-2018>.
- 15 685 (19) Huang, R.-J.; Cao, J.; Chen, Y.; Yang, L.; Shen, J.; You, Q.; Wang, K.; Lin, C.; Xu, W.; Gao, B.; et al.  
16 686 Organosulfates in Atmospheric Aerosol: Synthesis and Quantitative Analysis of PM<sub>2.5</sub> from Xi'an,  
17 687 Northwestern China. *Atmospheric Measurement Techniques* **2018**, *11* (6), 3447–3456.  
18 688 <https://doi.org/10.5194/amt-11-3447-2018>.
- 19 689 (20) Hettiyadura, A. P. S.; Jayarathne, T.; Baumann, K.; Goldstein, A. H.; de Gouw, J. A.; Koss, A.; Keutsch,  
20 690 F. N.; Skog, K.; Stone, E. A. Qualitative and Quantitative Analysis of Atmospheric Organosulfates in  
21 691 Centreville, Alabama. *Atmospheric Chemistry and Physics* **2017**, *17* (2), 1343–1359.  
22 692 <https://doi.org/10.5194/acp-17-1343-2017>.
- 23 693 (21) Chen, X.; Xie, M.; Hays, M. D.; Edgerton, E.; Schwede, D.; Walker, J. T. Characterization of Organic  
24 694 Nitrogen in Aerosols at a Forest Site in the Southern Appalachian Mountains. *Atmos. Chem. Phys.*  
25 695 **2018**, *18* (9), 6829–6846. <https://doi.org/10.5194/acp-18-6829-2018>.
- 26 696 (22) Surratt, J. D.; Gómez-González, Y.; Chan, A. W.; Vermeylen, R.; Shahgholi, M.; Kleindienst, T. E.; Edney,  
27 697 E. O.; Offenberg, J. H.; Lewandowski, M.; Jaoui, M. Organosulfate Formation in Biogenic Secondary  
28 698 Organic Aerosol. *The Journal of Physical Chemistry A* **2008**, *112* (36), 8345–8378.
- 29 699 (23) Iinuma, Y.; Böge, O.; Kahnt, A.; Herrmann, H. Laboratory Chamber Studies on the Formation of  
30 700 Organosulfates from Reactive Uptake of Monoterpene Oxides. *Physical Chemistry Chemical Physics*  
31 701 **2009**, *11* (36), 7985–7997.
- 32 702 (24) Duporte, G.; Flaud, P.-M.; Geneste, E.; Augagneur, S.; Pangu, E.; Lamkaddam, H.; Gratien, A.; Doussin,  
33 703 J.-F.; Budzinski, H.; Villenave, E. Experimental Study of the Formation of Organosulfates from  $\alpha$ -Pinene  
34 704 Oxidation. Part I: Product Identification, Formation Mechanisms and Effect of Relative Humidity. *The*  
35 705 *Journal of Physical Chemistry A* **2016**, *120* (40), 7909–7923.
- 36 706 (25) Chan, M. N.; Surratt, J. D.; Chan, A. W. H.; Schilling, K.; Offenberg, J. H.; Lewandowski, M.; Edney, E.  
37 707 O.; Kleindienst, T. E.; Jaoui, M.; Edgerton, E. S. Influence of Aerosol Acidity on the Chemical  
38 708 Composition of Secondary Organic Aerosol from  $\beta$ -Caryophyllene. *Atmospheric Chemistry and Physics*  
39 709 **2011**, *11* (4), 1735–1751.
- 40 710 (26) Riva, M.; Silva Barbosa, T. D.; Lin, Y.-H.; Stone, E. A.; Gold, A.; Surratt, J. D. Chemical Characterization  
41 711 of Organosulfates in Secondary Organic Aerosol Derived from the Photooxidation of Alkanes.  
42 712 *Atmospheric Chemistry and Physics* **2016**, *16* (17), 11001–11018.
- 43 713 (27) Tolocka, M. P.; Turpin, B. Contribution of Organosulfur Compounds to Organic Aerosol Mass.  
44 714 *Environmental science & technology* **2012**, *46* (15), 7978–7983.
- 45 715 (28) Pratt, K. A.; Fiddler, M. N.; Shepson, P. B.; Carlton, A. G.; Surratt, J. D. Organosulfates in Cloud Water  
46 716 above the Ozarks' Isoprene Source Region. *Atmospheric environment* **2013**, *77*, 231–238.
- 47 717 (29) Liggio, J.; Li, S.-M. Organosulfate Formation during the Uptake of Pinonaldehyde on Acidic Sulfate  
48 718 Aerosols. *Geophysical Research Letters* **2006**, *33* (13).
- 49 719 (30) Liggio, J.; Li, S.-M.; McLaren, R. Reactive Uptake of Glyoxal by Particulate Matter. *Journal of*  
50 720 *Geophysical Research: Atmospheres* **2005**, *110* (D10).
- 51 721 (31) Lin, Y.-H.; Zhang, Z.; Docherty, K. S.; Zhang, H.; Budisulistiorini, S. H.; Rubitschun, C. L.; Shaw, S. L.;  
52 722 Knipping, E. M.; Edgerton, E. S.; Kleindienst, T. E. Isoprene Epoxydiols as Precursors to Secondary  
53 723 Organic Aerosol Formation: Acid-Catalyzed Reactive Uptake Studies with Authentic Compounds.  
54 724 *Environmental science & technology* **2011**, *46* (1), 250–258.



1

2

- 3 725 (32) Nguyen, T. B.; Coggon, M. M.; Bates, K. H.; Zhang, X.; Schwantes, R. H.; Schilling, K. A.; Loza, C. L.;  
4 726 Flagan, R. C.; Wennberg, P. O.; Seinfeld, J. H. Organic Aerosol Formation from the Reactive Uptake of  
5 727 Isoprene Epoxydiols (IEPOX) onto Non-Acidified Inorganic Seeds. *Atmospheric Chemistry and Physics*  
6 728 **2014**, *14* (7), 3497–3510.
- 7 729 (33) Hu, K. S.; Darer, A. I.; Elrod, M. J. Thermodynamics and Kinetics of the Hydrolysis of Atmospherically  
8 730 Relevant Organonitrates and Organosulfates. *Atmospheric Chemistry and Physics* **2011**, *11* (16), 8307–  
9 731 8320. <https://doi.org/10.5194/acp-11-8307-2011>.
- 10 732 (34) Minerath, E. C.; Schultz, M. P.; Elrod, M. J. Kinetics of the Reactions of Isoprene-Derived Epoxides in  
11 733 Model Tropospheric Aerosol Solutions. *Environmental science & technology* **2009**, *43* (21), 8133–8139.
- 12 734 (35) Cortés, D. A.; Elrod, M. J. Kinetics of the Aqueous Phase Reactions of Atmospherically Relevant  
13 735 Monoterpene Epoxides. *Journal of Physical Chemistry A* **2017**, *121* (48), 9297–9305.  
14 736 <https://doi.org/10.1021/acs.jpca.7b09427>.
- 15 737 (36) Minerath, E. C.; Elrod, M. J. Assessing the Potential for Diol and Hydroxy Sulfate Ester Formation from  
16 738 the Reaction of Epoxides in Tropospheric Aerosols. *Environmental science & technology* **2009**, *43* (5),  
17 739 1386–1392.
- 18 740 (37) Minerath, E. C.; Casale, M. T.; Elrod, M. J. Kinetics Feasibility Study of Alcohol Sulfate Esterification  
19 741 Reactions in Tropospheric Aerosols. *Environmental science & technology* **2008**, *42* (12), 4410–4415.
- 20 742 (38) Bleier, D. B.; Elrod, M. J. Kinetics and Thermodynamics of Atmospherically Relevant Aqueous Phase  
21 743 Reactions of  $\alpha$ -Pinene Oxide. *The Journal of Physical Chemistry A* **2013**, *117* (20), 4223–4232.
- 22 744 (39) Surratt, J. D.; Chan, A. W.; Eddingsaas, N. C.; Chan, M.; Loza, C. L.; Kwan, A. J.; Hersey, S. P.; Flagan, R.  
23 745 C.; Wennberg, P. O.; Seinfeld, J. H. Reactive Intermediates Revealed in Secondary Organic Aerosol  
24 746 Formation from Isoprene. *Proceedings of the National Academy of Sciences* **2010**, *107* (15), 6640–  
25 747 6645.
- 26 748 (40) Nozière, B.; Ekström, S.; Alsberg, T.; Holmström, S. Radical-Initiated Formation of Organosulfates and  
27 749 Surfactants in Atmospheric Aerosols: ORGANOSULFATES AND SURFACTANTS IN AEROSOLS.  
28 750 *Geophysical Research Letters* **2010**, *37* (5), n/a-n/a. <https://doi.org/10.1029/2009GL041683>.
- 29 751 (41) Perri, M. J.; Lim, Y. B.; Seitzinger, S. P.; Turpin, B. J. Organosulfates from Glycolaldehyde in Aqueous  
30 752 Aerosols and Clouds: Laboratory Studies. *Atmospheric Environment* **2010**, *44* (21–22), 2658–2664.  
31 753 <https://doi.org/10.1016/j.atmosenv.2010.03.031>.
- 32 754 (42) Eddingsaas, N. C.; VanderVelde, D. G.; Wennberg, P. O. Kinetics and Products of the Acid-Catalyzed  
33 755 Ring-Opening of Atmospherically Relevant Butyl Epoxy Alcohols. *The Journal of Physical Chemistry A*  
34 756 **2010**, *114* (31), 8106–8113. <https://doi.org/10.1021/jp103907c>.
- 35 757 (43) Wang, J.; Doussin, J. F.; Perrier, S.; Perraudin, E.; Katrib, Y.; Pangu, E.; Picquet-Varrault, B. Design of a  
36 758 New Multi-Phase Experimental Simulation Chamber for Atmospheric Photosmog, Aerosol and Cloud  
37 759 Chemistry Research. *Atmospheric Measurement Techniques* **2011**, *4* (11), 2465.
- 38 760 (44) Lamkaddam, H.; Gratien, A.; Pangu, E.; Cazaunau, M.; Picquet-Varrault, B.; Doussin, J.-F. High-NO<sub>x</sub>  
39 761 Photooxidation of *n*-Dodecane: Temperature Dependence of SOA Formation. *Environmental Science*  
40 762 *& Technology* **2017**, *51* (1), 192–201. <https://doi.org/10.1021/acs.est.6b03821>.
- 41 763 (45) K. Lai, A. C.; Nazaroff, W. W. MODELING INDOOR PARTICLE DEPOSITION FROM TURBULENT FLOW  
42 764 ONTO SMOOTH SURFACES. *Journal of Aerosol Science* **2000**, *31* (4), 463–476.  
43 765 [https://doi.org/10.1016/S0021-8502\(99\)00536-4](https://doi.org/10.1016/S0021-8502(99)00536-4).
- 44 766 (46) Kristensen, K.; Glasius, M. Organosulfates and Oxidation Products from Biogenic Hydrocarbons in Fine  
45 767 Aerosols from a Forest in North West Europe during Spring. *Atmospheric environment* **2011**, *45* (27),  
46 768 4546–4556.
- 47 769 (47) Iinuma, Y.; Kahnt, A.; Mutzel, A.; Böge, O.; Herrmann, H. Ozone-Driven Secondary Organic Aerosol  
48 770 Production Chain. *Environmental science & technology* **2013**, *47* (8), 3639–3647.
- 49 771 (48) Lal, V.; Khalizov, A. F.; Lin, Y.; Galvan, M. D.; Connell, B. T.; Zhang, R. Heterogeneous Reactions of  
50 772 Epoxides in Acidic Media. *The Journal of Physical Chemistry A* **2012**, *116* (24), 6078–6090.
- 51 773 (49) Wang, Y.; Ma, Y.; Li, X.; Kuang, B. Y.; Huang C.; Tog, R.; Yu, J. Z. Monoterpene and Sesquiterpene  $\alpha$ -  
52 774 Hydroxy Organosulfates: Synthesis, MS/MS Characteristics, and Ambient Presence. *Environmental*  
53 775 *science & technology* **2019**, *53*, 12278-12290.
- 54 776
- 55 777
- 56 778
- 57 779
- 58 780
- 59 781
- 60 782

1  
2  
3  
4  
5  
6  
7  
8  
9  
10  
11  
12  
13  
14  
15  
16  
17  
18  
19  
20  
21  
22  
23  
24  
25  
26  
27  
28  
29  
30  
31  
32  
33  
34  
35  
36  
37  
38  
39  
40  
41  
42  
43  
44  
45  
46  
47  
48  
49  
50  
51  
52  
53  
54  
55  
56  
57  
58  
59  
60

- (50) Lim, Y. B.; Ziemann, P. J. Kinetics of the Heterogeneous Conversion of 1,4-Hydroxycarbonyls to Cyclic Hemiacetals and Dihydrofurans on Organic Aerosol Particles. *Phys. Chem. Chem. Phys.* **2009**, *11* (36), 8029. <https://doi.org/10.1039/b904333k>.
- (51) Chan, K. M.; Huang, D. D.; Li, Y. J.; Chan, M. N.; Seinfeld, J. H.; Chan, C. K. Oligomeric Products and Formation Mechanisms from Acid-Catalyzed Reactions of Methyl Vinyl Ketone on Acidic Sulfate Particles. *J Atmos Chem* **2013**, *70* (1), 1–18. <https://doi.org/10.1007/s10874-013-9248-7>.
- (52) Khalizov, A. F.; Zhang, R.; Zhang, D.; Xue, H.; Pagels, J.; McMurry, P. H. Formation of Highly Hygroscopic Soot Aerosols upon Internal Mixing with Sulfuric Acid Vapor. *Journal of Geophysical Research Atmospheres* **2009**, *114* (5). <https://doi.org/10.1029/2008JD010595>.
- (53) Drozd, G. T.; Woo, J. L.; McNeill, V. F. Self-Limited Uptake of  $\alpha$ -Pinene Oxide to Acidic Aerosol: The Effects of Liquid–Liquid Phase Separation and Implications for the Formation of Secondary Organic Aerosol and Organosulfates from Epoxides. *Atmospheric Chemistry and Physics* **2013**, *13* (16), 8255–8263.
- (54) Stekrova, M.; Kumar, N.; Aho, A.; Sinev, I.; Grünert, W.; Dahl, J.; Roine, J.; Arzumanov, S. S.; Mäki-Arvela, P.; Murzin, D. Y. Isomerization of  $\alpha$ -Pinene Oxide Using Fe-Supported Catalysts: Selective Synthesis of Campholenic Aldehyde. *Applied Catalysis A: General* **2014**, *470*, 162–176.
- (55) Gaston, C. J.; Riedel, T. P.; Zhang, Z.; Gold, A.; Surratt, J. D.; Thornton, J. A. Reactive Uptake of an Isoprene-Derived Epoxydiol to Submicron Aerosol Particles. *Environmental science & technology* **2014**, *48* (19), 11178–11186.
- (56) Meng, Z.; Seinfeld, J. H.; Saxena, P.; Kim, Y. P. Atmospheric Gas-Aerosol Equilibrium: IV. Thermodynamics of Carbonates. *Aerosol Science and Technology* **1995**, *23* (2), 131–154.
- (57) Kerminen, V.-M.; Hillamo, R.; Teinilä, K.; Pakkanen, T.; Allegrini, I.; Sparapani, R. Ion Balances of Size-Resolved Tropospheric Aerosol Samples: Implications for the Acidity and Atmospheric Processing of Aerosols. *Atmospheric Environment* **2001**, *35* (31), 5255–5265.
- (58) Guo, H.; Xu, L.; Bougiatioti, A.; Cerully, K. M.; Capps, S. L.; Hite Jr., J. R.; Carlton, A. G.; Lee, S.-H.; Bergin, M. H.; Ng, N. L.; et al. Fine-Particle Water and PH in the Southeastern United States. *Atmos. Chem. Phys.* **2015**, *15* (9), 5211–5228. <https://doi.org/10.5194/acp-15-5211-2015>.
- (59) Riva, M.; Bell, D. M.; Hansen, A.-M. K.; Drozd, G. T.; Zhang, Z.; Gold, A.; Imre, D.; Surratt, J. D.; Glasius, M.; Zelenyuk, A. Effect of Organic Coatings, Humidity and Aerosol Acidity on Multiphase Chemistry of Isoprene Epoxydiols. *Environ. Sci. Technol.* **2016**, *50* (11), 5580–5588. <https://doi.org/10.1021/acs.est.5b06050>.

809 **Table of Contents Image**

810

